AD658846

STRESSES IN SKIN PANELS SUBJECTED TO RANDOM ACOUSTIC LOADING

BRIAN L. CLARKSON

INSTITUTE OF SOUND AND VIBRATION RESEARCH
UNIVERSITY OF SOUTHAMPTON

TECHNICAL REPORT AFML-TR-67-199

JUNE 1967

AIR FORCE MATERIALS LABORATORY
RESEARCH AND TECHNOLOGY DIVISION
AIR FORCE SYSTEMS COMMAND
WRIGHT-PATTERSON AIR FORCE BASE, OHIO

NOTICES

When Government drawings, specifications, or other data are used for any purpose other than in connection with a definitely related Government procurement operation, the United States Government thereby incurs no responsibility nor any obligation whatsoever; and the fact that the Government may have formulated, furnished, or in any way supplied the said drawings, specifications, or other data, is not to be regarded by implication or otherwise as in any manner licensing the holder or any other person or corporation, or conveying any rights or permission to manufacture, use, or sell any patented invention that may in any way be related thereto.

Copies of this report should not be returned to the Research and Technology Division unless return is required by security considerations, contractual obligations, or notice on a specific document.

STRESSES IN SKIN PANELS SUBJECTED TO RANDOM ACOUSTIC LOADING

BRIAN L. CLARKSON

INSTITUTE OF SOUND AND VIBRATION RESEARCH
UNIVERSITY OF SOUTHAMPTON

ABSTRACT

      This report summarises the fully documented experimental data
which is available on the stresses induced in typical aircraft structure
by jet noise at take off. The experimental values are compared with a
design procedure based on a single degree of freedom analysis and the
method is extended for application to control surfaces and to integrally
stiffened skin panels. The estimates are generally within a factor of
two of the measured values. The relatively new phenomenon of shock cell
noise is introduced and a typical result for the variation of r.m.s. stress
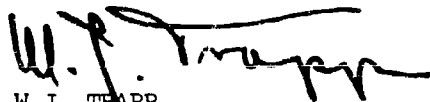during take off and climb is discussed.

CONTENTS

1. Introduction

As a result of the failure of parts of the airframe on several types of aircraft having high intensity acoustic environments, the military and civil certification authorities are requiring assurances that new designs have adequate strength to resist the acoustic loads. In most cases failures have been detected early enough to prevent serious impairment of the aircraft's structural strength. This, however, has led to unsatisfactory maintenance and inspection requirements and there is also the possibility of more serious failures arising from the extension of undetected damage. The purpose of this report is to review the test data available and to present a design procedure for structure in the region of high noise levels. The full theoretical treatment is impossible to apply but an approximation is presented and the predicted results are compared with the experimental values.

A detailed analysis of the response of some full scale aircraft structures to jet noise has been given by Clarkson and Ford[1,2] and by Schelderup.[3] Many other full scale measurements have been made by the aircraft manufacturers but few of these results have been fully analysed and published. Such data as is available is summarised in Section 4. It is hoped that companies with further data available will check their results against the design method presented here and forward the results to the author to enable a wider range of applications to be covered.

The complete theoretical analysis of the response of a shell type structure to distributed random loads such as those produced by an acoustic environment has been developed by Powell[4]. This is based on the normal mode method and hence is a very lengthy computational procedure. In fact only a simplified model of the structure can be considered with present day computers. However the method brings out the important parameters and forms a basis for more detailed design optimisation. At the other end of the scale a considerable amount of work has been done by the Douglas Aircraft Company on the development of a design method[5]. The aim of this work is to produce a single comprehensive design chart for each type of construction. Then, knowing the noise level and required life, the designer reads off the appropriate skin dimensions. Whilst being an ideal form of presentation from the

1

designer's point of view it restricts the designers freedom of action.
For example he cannot easily use his own fatigue or stress response data.
The method presented in this report is essentially the same as that
proposed in the Douglas work but the procedure is split up into the
several steps. Then at each step the designer can use his own or the
latest published data. This report also sets out to check the accuracy
of the method by comparing it with test results from a wide range of
structures.

The majority of this report is concentrated on the stress
response of typical structures to jet noise but in the later sections the
fatigue aspects are briefly considered. The recently observed
phenomenon of shock cell noise which can give in-flight stress levels as
high as or even higher than the levels produced by the maximum engine
thrust on the ground is also discussed. This is particularly important
when making estimates of fatigue life as the exposure to significant
stress levels can be increased from 30 seconds to one hour or so per
flight in the worst condition.

2. General Theory

When a continuous structure, such as an aircraft fuselage or
control surface, is excited by broad frequency band random forces the
resulting vibration can be treated as the summation of responses in a
relatively large number of modes producing an overall picture of broad
band response. In some types of structure a few or even a single mode
may predominate but in general the broader band response situation must
be considered.

Using the normal mode method, the spectral density of the
displacement at any point x_1 on the surface of the structure can be
expressed in terms of the normal modes of the structure and the
characteristics of the pressure field as:

$$G(x_1 \omega) = \sum_{r=1}^{\infty} \sum_{s=1}^{\infty} \frac{f_r(x_1) f_s(x_1) \int_A \int_A f_r(x_A) f_s(x_B) G_p(x_A x_B \omega) \, dA \, dA}{M_r(\omega_r^2 - \omega^2 + i\eta_r \omega_2^2) M_s(\omega_s^2 - \omega^2 - i\eta_s \omega_s^2)}$$

..1.

Where $\underset{\sim}{x}$ are vectors defining the position of points on the surface

$$f_r(\underset{\sim}{x}) = \text{mode shape}$$

$$M_r = \text{generalised mass}$$

$$\omega_r = \text{undamped natural frequency}$$

$$\eta_r = \text{damping factor (hysteretic damping)}$$

$$G_p(\underset{\sim}{x}_A \underset{\sim}{x}_B \omega) = \text{cross spectral density of the pressure at } \underset{\sim}{x}_A \text{ and } \underset{\sim}{x}_B$$

This result is based on the work of Powell[4] and has recently been given in terms of receptances by Robson[6] as:

$$G(\underset{\sim}{x}_1 \omega) = \int_A \int_A \alpha_{1A}^* \, \alpha_{1B} \, G_p(x_A x_B \, \omega) \, dA \, dA \qquad ..2.$$

where the receptance α_{1A} is the displacement at x_1 caused by a a unit amplitude harmonic force of frequency ω applied at x_A.

The first expression shows all the parameters which are involved whereas the second expression may be useful if experimentally determined values of receptance are available.

Equation (1) shows that in addition to the normal modes, undamped natural frequencies, and modal damping factors it is also necessary to know the cross spectral density of the acoustic pressures. In many cases it is reasonable to assume a homogeneous pressure field in which situation the cross spectral density is only a function of the separation between the points $\underset{\sim}{x}_A$ and $\underset{\sim}{x}_B$.

Thus we can write

$$G_p(\underset{\sim}{x}_A, \underset{\sim}{x}_B, \omega) = G_p(\underset{\sim}{x}_B - \underset{\sim}{x}_A, \omega) = G_p(\underset{\sim}{\xi}, \omega) \qquad ..3.$$

It is often more convenient to split this up further into:

$$G_p(\underset{\sim}{\xi}, \omega) = G_p(\omega)\rho_\omega(\underset{\sim}{\xi}) \qquad ..4.$$

where $G_p(\omega)$ is the direct spectral density of the pressures (now assumed to be the same at each point on the structure) and $\rho_\omega(\underset{\sim}{\xi})$ is the correlation coefficient for the components of the pressures in the

3

narrow frequency band $\omega - \frac{\Delta\omega}{2}$ to $\omega + \frac{\Delta\omega}{2}$ at two points separated by the distance ξ. This narrow band space correlation has been normalised by dividing by the spectral density of the pressure to give a correlation coefficient ρ. The advantage of this form of representation is that in the case of jet noise, the narrow band space correlation coefficient only changes slowly with frequency and thus reasonable estimates can be made from a few measurements. In most aircraft configurations the direct spectral density of the noise pressures varies considerably over the surface of the structure as a result of the strong directional characteristics of jet noise. However if one is considering smaller sections of structure such as an individual skin plate or a small array of plates it might be reasonable to assume a constant pressure level over the complete surface of interest.

A great simplification can be made if it is assumed that the space correlation coefficient is a Dirac delta function in space. The double area integration of equation (1) reduces to a single integration of the square of the mode shape. This then cancels out with one of the generalised mass terms. Also the double series summation reduces to a single series summation. This assumption has been made in several theoretical studies of the response of structures to boundary layer pressure fluctuations. In most jet noise situations, however, the spatial scale of the pressure correlation coefficient is of the same order as the mode wavelength and thus cannot be treated as a delta function. In these cases there is coupling of the modal responses due to the pressure cross correlation term but in practice, when the damping is usually very small, the reciprocal of the frequency function in the denominator will only have non zero values at frequencies close to the natural frequency of each mode. Thus the cross terms will be very small except when natural frequencies occur very close together.

An investigation of the effect of the cross terms has been made by Mercer[7] who considered the case of a continuous beam resting on many supports and excited by acoustic pressures. In the case showing maximum coupling the cross terms only contributed an additional 20 per cent to the overall r.m.s. response level. In more typical cases the contribution was of the order of 5 to 10 per cent. Thus only relatively small errors are likely to arise from the neglect of the cross terms.

4

However, even if the cross terms are small a large number of direct terms will be significant if the excitation forces have a broad frequency bandwidth. Thus in cases of broad band excitation the computation of response using equation (1) for all the modes having frequencies in the bandwidth of the excitation is prohibitively lengthy. Thus there is great interest in realistic simplification of the structure and also in measurements of the overall receptances as used in equation (2).

If the cross terms are neglected the spectral density of displacement can be rewritten as:

$$G(\underset{\sim}{x}_1\,\omega) = \sum_{r=1}^{\infty} \frac{f_r^2(\underset{\sim}{x}_1)\,\int_A\int_A f_r(\underset{\sim}{x}_A)f_r(\underset{\sim}{x}_B)G_p(\underset{\sim}{x}_A\underset{\sim}{x}_B\,\omega)\,dA\,dA}{M_r^2\left[(\omega_r^2 - \omega^2)^2 + \eta_r^2\omega_r^4\right]} \quad ..5.$$

The mean square value of the overall displacement at $\underset{\sim}{x}_1$ is obtained by integrating equation 5 over all frequencies. Thus

$$\overline{y^2(t)} = \int_0^{\infty} G(\underset{\sim}{x}_1\,\omega)\,d\omega \quad ..6.$$

If the modes are well separated in frequency, the damping is small, and the spectral density is changing very slowly with frequency then the frequency integration can be performed separately for each mode and equation 6 can then be written as:

$$\overline{y^2(t)} = \sum_{r=1}^{N} \frac{\pi}{2\omega_r^3\eta_r}\,\frac{f_r^2(\underset{\sim}{x}_1)}{M_r^2}\int_A\int_A f_r(\underset{\sim}{x}_A)f_r(\underset{\sim}{x}_B)G_p(\underset{\sim}{x}_A\underset{\sim}{x}_B\omega_r)\,dA\,dA \quad ..7.$$

3. Simplified Theory of Response

The classical theory for the complete description of response, as outlined in section 2, is too complicated to be used in design. For the purpose of design it is suggested that a very much simplified version be used. This simplified theory is derived on the assumption that the major part of the response results from the contribution of one predominant mode. The tests on full scale structures have shown that in certain types of structure (usually large skin plates) the response spectrum may only have one major peak

resulting from one mode of vibration. In other structure such as control surface skin plating there may be many peaks in the response spectrum. Even in this case, however, the simple theory gives a reasonable estimate of the overall stress level. Nevertheless it is clearly necessary to examine the application of the theory in a wide range of structures to establish the limitations.

3.1. Single Mode Response

Assuming only one significant mode of response the mean square level of displacement is derived from equation 7 as:

$$\overline{y^2(t)} = \frac{\pi}{2\omega_r^3 \eta_r} \frac{f_r^2(x_1)}{M_r^2} \int_A \int_A f_r(x_A) f_r(x_B) G_p(x_A x_B \omega_r) dA \, dA \quad ..8.$$

where r is the predominant mode – usually the first mode. This now eliminates the mode summation and simplifies the structure to a set of independent plates responding in their fundamental mode only.

The second major simplification is to assume that the pressures are exactly in phase over the whole plate. Equation 8 then becomes:

$$\overline{y^2(t)} = \frac{\pi}{2\omega_r^3 \eta_r} \frac{f_r^2(x_1)}{M_r^2} \left[\int_A f_r(x_A) dA \right]^2 G_p(\omega_r) \quad ..9.$$

This can be written in terms of the displacement response of the plate to a uniform static pressure of unit magnitude. The static displacement y_o at x_1 is given by

$$y_o = \frac{\int_A f_r(x_A) dA}{\omega_r^2 M_r} \cdot f_r(x_1)$$

Thus equation 9 can be written as:

$$\overline{y^2(t)} = \frac{\pi}{2\eta_r} \omega_r G_p(\omega_r) y_o^2 \quad ..10.$$

6

The more usual expression for the mean square stress can be written in terms of the viscous damping ratio δ and frequency in cycles per second f, as:

$$\overline{\sigma^2(t)} \; = \; \frac{\pi}{4\delta} \; f_r \; G_p(f_r) \; \sigma_o^2 \qquad\qquad ..11.$$

where σ_o is the stress at the point of interest due to a uniform static pressure of unit magnitude. This expression was first derived from the consideration of a single degree of freedom system by Miles[8].

3.2. Application to Flat Plates

Equation 11 can be applied directly to the case of a flat plate excited by random acoustic pressures. The spectral density $G_p(f_r)$ should be determined for the acoustic loading at the fundamental frequency of the plate. The damping ratio δ is not generally known accurately but is likely to be in the range 0.01 to 0.02.

In aircraft structures the individual plates are connected to other plates or stiffeners at their boundaries and thus have an elastic restraint at their edges. As a result of this the frequency of the fundamental mode of vibration lies somewhere between the limiting cases given by either simply supported edges or fully fixed edges. Figure 1 gives the frequencies of these two limits for plates of different dimensions. The cross hatching between the bounds is there to imply that in practice any one plate will have a frequency somewhere in the cross hatched region. The basis assumed for the design method is the fully fixed edge condition.

Assuming fully fixed edge conditions the variation of the stress parameter σ_o with aspect ratio for the stress at the edge and at the centre of the plate is shown in figure 2. This has been obtained from Timoshenko and Woinowsky-Krieger[9].

On the assumption that only one mode of vibration is excited by the noise we can use the simplified equation (11) to study the effects of changes in plate properties on the r.m.s. stress. If the plate aspect ratio is kept constant the natural frequency of the fundamental mode of vibration is proportional to t/b^2 and the static stress parameter is proportional to $\dfrac{b^2}{t^2}$ where t is the thickness and b

7

is the short dimension. Then if it is assumed that the spectral density of the pressure is the same at the new natural frequency, the r.m.s. stress varies in the following way:

$$\sqrt{\overline{\sigma^2(t)}} \sim \delta^{1/2} b t^{3/2} \qquad ..12.$$

This gives a very rough guide as to how the r.m.s. stress increases with increase in plate width and decreases with increase in plate thickness.

In many practical cases however failure occurs initially in the attachment cleats etc. which fix the skin to the supporting frames of ribs. The loads coming on to these attachments are due to the inertia force from the vibrating skin. The mean square of the inertia force is proportional to

$$(\text{skin mass})^2 \times f_r^4 \times \overline{y^2(t)}$$

where $\overline{y^2(t)}$ is the mean square displacement of the centre, say, and can be derived from equation (10):

$$\overline{y^2(t)} = \frac{\pi}{4\delta} \, f_r \, G_p(f_r) y_o^2 \qquad ..13.$$

Now for a fixed aspect ratio, y_o is proportional to $\dfrac{b^4}{t^3}$ and the skin mass is proportional to $b\,t$. Thus the mean square inertia force is proportional to

$$(b\,t)^2 \times \left(\frac{t}{b^2}\right)^4 \times \frac{t}{b^2} \times \left(\frac{b^4}{t^3}\right)^2 = t$$

Thus the root mean square inertia force is proportional to $t^{1/2}$ and <u>increases</u> with increase in plate thickness.

The accuracy of these approximations is discussed in section 4.

3.3. Application to Control Surfaces

In the case of control surfaces, two skins are attached

8

together by ribs and thus both skins and ribs vibrate because of the mechanical coupling between them. Even when the sound pressures are much greater on one side of the control surface, due to acoustic shielding, the stresses in both skins are very similar. These types of structure are not so amenable to the simple form of analysis outlined in section 3.1. as now the sound energy incident on one skin, minus the reflected energy, is absorbed by two vibrating skins and the inter-connecting ribs. Consequently the stress level must be less than half and is possibly about one third of that which would have been induced in a single plate. Making the assumption that the stress is reduced to one third of the single plate case the root mean square stress is then given by:

$$\sqrt{\overline{\sigma^2(t)}} = \frac{1}{3}\left[\frac{\pi}{4\delta} \; f_r \; G_p(f_r) \; \sigma_o^2\right]^{\frac{1}{2}} \qquad ..14.$$

This generally applies to tailplanes, elevators and flaps.

Where there is incident sound energy on both skins, as may be the case for fins and rudders, the overall excitation level is increased by approximately 3dB (intensity has been doubled). Thus the stress would be 1.4 times higher than for the single sided exposure. Equation 14 should therefore be modified to read:

$$\sqrt{\overline{\sigma^2(t)}} = \frac{1.4}{3}\left[\frac{\pi}{4\delta} \cdot f_r \; G_p(f_r)\sigma_o^2\right]^{\frac{1}{2}} \qquad ..15$$

This factor of 1.4 has been shown to be reasonable in the tests reported in reference 3. The experimental results discussed in section 4 show that this simple relationship gives a reasonably good estimate of the stresses in the control surface skin plating of the aircraft where response data is available.

3.4. Application to Integrally Stiffened Skins

The theory outlined in section 3.2. can be applied to skin panels which have substantial stiffening members. Closed section stiffeners for example provide a relatively rigid boundary to the individual plates which make up the stiffened panel. In these cases

9

the assumption that the individual plates are fully fixed around their
edges is a reasonable approximation. However in the case of integrally
stiffened panels the individual plates between stiffeners are generally
narrower and the machined stiffeners themselves are less rigid than in
the equivalent built up structure. As a result the individual plates
are effectively much stiffer and the supports are relatively weaker.
In this situation the stiffeners are unable to provide an effectively
rigid boundary to the individual plates and they bend a significant
amount. Figure 3 illustrates the effect of this on the lowest natural
frequency of an integrally stiffened panel as computed from Lin's
theory[10]. In this case the plates are 3" wide and 14" long. For very
small plate thicknesses the lowest frequency is close to the fully fixed
frequency for the plate but as the thickness increases the frequency
approaches the frequency associated with the bending of the stiffener. At
typical aircraft dimensions (thickness in the range 0.05" to 0.08") the
lowest frequency is close to the stiffener bending frequency. It is clear
that in these cases the fully fixed plate approximation would be
considerably in error if used in estimations of the natural frequencies and
also the stresses induced by acoustic loads.

Modes Shapes and Natural Frequencies

A better approximation in this case is to allow for the
flexibility of the stiffeners supporting the sides of the plate. The
model taken for this approximation is a panel made up of many plates as
shown in figure 4a. The edges of the panel are assumed to be fully fixed
and the number of individual plates is assumed to be sufficiently great for
the centre plate to be unaffected by the number of plates in the panel.
This latter assumption means that an approximation to the fundamental mode
can be determined from a consideration of a single plate plus its
supporting stiffeners. The aim of the approximate solution is to obtain
estimates of the natural frequency of the fundamental mode and also values
for the stress parameter σ_o for different relative stiffnesses of plate
and stiffener. The approximate solution is based on the Rayleigh-Ritz
Energy Method.

The single plate element of the panel is shown in figure 4b and
for the energy method it is necessary to consider the strain energy and
the kinetic energy of one plate plus one beam (stiffener). Using the

notation shown in the figure a suitable lateral displacement function
fitting the boundary conditions during free vibration is:

$$w = A_o W \sin \omega t$$

where ω is the natural frequency of the fundamental mode and

$$W = \left(1 + \cos \frac{2\pi y}{a}\right) + K\left(1 + \cos \frac{2\pi x}{b}\right)\left(1 + \cos \frac{2\pi y}{a}\right) \qquad ..16.$$

and the constant K will depend on the relative stiffness of the plate
and beam support.

During free vibration the maximum strain energy is given by:

$$V = A_o^2 \frac{D}{2} \int_{-a/2}^{a/2} \int_{-b/2}^{b/2} \left\{ \left(\frac{\partial^2 W}{\partial x^2}\right)^2 + \left(\frac{\partial^2 W}{\partial y^2}\right)^2 + 2\nu \frac{\partial^2 W}{\partial x^2} \cdot \frac{\partial^2 W}{\partial y^2} + 2(1-\nu)\left(\frac{\partial^2 W}{\partial x \partial y}\right)^2 \right\} dxdy$$

$$+ A_o^2 \frac{EI}{2} \int_{-a/2}^{a/2} \left(\frac{\partial^2 W}{\partial y^2}\right)^2_{x=b/2} dy \qquad ..17.$$

and the maximum kinetic energy is given by:

$$T = A_o^2 \frac{\rho t}{2} \omega^2 \int_{-a/2}^{a/2} \int_{-b/2}^{b/2} W^2 \, dxdy + A_o^2 \rho_B \frac{\omega^2}{2} \int_{-a/2}^{a/2} (W)^2_{x=b/2} \, dy$$

$$..18.$$

Then ω can be found by equating the maximum strain energy to the maximum
kinetic energy in undamped free vibration. Thus

$$\omega^2 = \frac{V}{T'} \qquad ..19.$$

where $\qquad T' = T/\omega^2$

We must now choose the constant K to be such as to give a minimum value
of ω. To do this we write

11

$$\frac{\partial \omega^2}{\partial K} = 0$$

or
$$T' \frac{\partial V}{\partial K} - V \frac{\partial T'}{\partial K} = C \qquad ..20.$$

or alternatively
$$\frac{\partial V}{\partial K} - \omega^2 \frac{\partial T'}{\partial K} = 0 \qquad ..21.$$

Thus the constant K can be determined from equation 20 and then the natural frequency ω can be obtained from either equation 19 or equation 21.

Substituting the displacement function given by equation 16 into the expression for V and T' we obtain the following results:

$$V = A_o^2 \frac{2\pi^4}{a^3} \left[K^2 \frac{D}{b^3} (3a^4 + 3b^4 + 2a^2b^2) + 4Kb + 2(Db + EI) \right] \qquad ..22.$$

$$\frac{\partial V}{\partial K} = A_o^2 \frac{2\pi^4}{a^3} \left[2K \frac{D}{b^3} (3a^4 + 3b^4 + 2a^2b^2) + 4Db \right] \qquad ..23.$$

$$T' = A_o^2 \frac{3}{4} a \left[\rho tb \left(\frac{3K^2}{2} + 2K + 1 \right) + \rho_B \right] \qquad ..24.$$

$$\frac{\partial T'}{\partial K} = A_o^2 \frac{3}{4} a \quad \rho tb (3K + 2) \qquad ..25.$$

The equation for K (20) then becomes:

$$K^2 \, 2\rho tb \left[A - 3Db \right] + K \left[2A\rho tb - 6\rho tb(Db + EI) + 2\rho_B A \right]$$

$$+ 4 \left[Db\rho_B - \rho tb \, EI \right] = 0 \qquad ..26.$$

12

where $A = \dfrac{D}{b^3} (3a^4 + 3b^4 + 2a^2b^2)$

The equation for frequency ω (21) becomes:

$$\omega^2 = \frac{8\,\pi^4\,(2AK + 4Db)}{3\,a^4\,\rho tb(3K + 2)} \qquad ..27.$$

Stresses

The stress parameter σ_o can now be obtained by computing the deflection of the plate when subjected to a unit static pressure. Using the energy method we can equate the work done by the static pressure to the maximum strain energy in the plate system (equation 22).

The work done by the unit static pressure is

$$U = \frac{1}{2} \int_{-a/2}^{a/b} \int_{-b/2}^{b/2} A_o W \, dx \, dy$$

$$= \frac{A_o}{2} \; ab(1 + K) \qquad ..28.$$

Equating this with the value for V given by equation 22 we have:

$$A_o = \frac{a^4 b(1 + K)}{4\pi^4 \left[K^2 + 4Y\, Db + 2(Db + EI) \right]} \qquad ..29.$$

The individual plates generally have a high aspect ratio a/b and thus we are primarily interested in the surface stresses at the centre of the plate and at the centre of each edge in the direction normal to the edge. Referring to figure 4b these requirements are:

13

1. σ_x at $x = 0$, $y = 0$, $z = t/2$

2. σ_x at $x = b/2$, $y = 0$, $z = t/2$

3. σ_y at $x = 0$, $y = a/2$, $z = t/2$

And the maximum stress in the stiffening beam is given by:

4. σ_y at $x = b/2$, $y = 0$, $z = d/2$

These stresses can be determined by substituting the displacement function into the following standard expressions for plate stresses:

$$\sigma_x = \frac{Ez}{(1 - \nu^2)} \left\{ \frac{\partial^2 w}{\partial x^2} + \nu \frac{\partial^2 w}{\partial y^2} \right\}$$

$$\sigma_y = \frac{Ez}{(1 - \nu^2)} \left\{ \frac{\partial^2 w}{\partial y^2} + \frac{\partial^2 w}{\partial x^2} \right\}$$

The maximum stresses at the extreme amplitude position and the approximations for high aspect ratio plates then become:

1. $x = 0$, $y = 0$

$$\sigma_x = - A_o \frac{Et}{2(1 - \nu^2)} \cdot \frac{4\pi^2}{a^2 b^2} \{2a\, K + \nu t^2(1 + 2K)\}$$

$$\cong - A_o \frac{Et}{(1 - \nu^2)} \, 4 \frac{\pi^2 K}{t^2} \qquad\qquad ..30.$$

2. $x = + b/2$ $y = 0$

$$\sigma_x = + A_o \frac{Et}{2(1 - \nu^2)} \, \frac{4\pi^2}{a^2 b^2} \{2a\, K - \nu^2 b^2\}$$

$$\cong + A_o \frac{Et}{(1 - \nu^2)} \, \frac{4\pi^2 K}{b^2} \qquad\qquad ..31.$$

14

3. $x = 0$ $y = + a/2$

$$\sigma_y = + A_o \frac{Et}{2(1 - \nu^2)} \frac{4\pi^2}{a^2} (1 + 2K) \qquad ..32.$$

4.   Beam, $x = + b/2$ $y = 0$

$$\sigma_y = - A_o \frac{Ed}{2} . \frac{4\pi^2}{a^2} \qquad ..33.$$

The equations 30 to 33 can be used to evaluate the stress parameters σ_o after A_o and K have been determined.

4. Test Results and Discussion

In many tests which have been made to date on aircraft structure subjected to jet noise the full information necessary to carry out stress level estimates has not been obtained.   In some cases the noise levels have not been measured whilst in other cases the noise levels have been measured at a different time from the stress level measurements. In some cases the noise level measurements are presented as octave band levels whereas in most recent cases they are given as one third octave levels.   Usually r.m.s. stress levels have been measured but in a few cases the measurement consisted of choosing the largest peak in a relatively long record and measuring its amplitude.   With this latter kind of measurement the result is approximately three times the r.m.s. level.

Little fully documented data on stress response for typical structures is available in the literature.   Most of the information is in the form of company test reports which have not been published.   In this report all the information available to the author is presented and compared with estimates based on the simplified theory outlined in the previous section.   Details of the structures and any special aspects of the tests are given in the Appendix for each aircraft and test specimen for which results are available.

The estimates for single flat plates and for control surfaces are relatively simple to make but determination of frequency and stress

15

parameter σ_o for the stiffened panels is a more lengthy process. For single flat plates the r.m.s. stress estimate is obtained from equation 11 as:

$$\sqrt{\overline{\sigma^2(t)}} = \left[\frac{\pi}{4\delta} \ f_r \ G_p(f_r) \right]^{\frac{1}{2}} \sigma_o \qquad ..34.$$

Few reliable measurements of damping are available in the test results and so an assumed value of 0.017 is taken in the evaluation of equation 34. This is a reasonable value in the light of measurements made on typical structure. (See reference 1 for example). It is also useful to compute a spectrum level of noise (in dB) and then convert this into lb/ft² and use this in the estimation procedure. We then have

$$\sqrt{\overline{\sigma^2(t)}} = 0.047 \ S_{PL} \ f_r^{\frac{1}{2}} \ \sigma_o \qquad ..35.$$

where S_{PL} is the noise spectrum level in lb/ft² at the plate fundamental natural frequency.

Equation 35 now becomes the basic equation for the three types of structure considered in section 3. It is used as it stands with f_r and σ_o being obtained from figures 1 and 2 for flat plates. For application to control surfaces a factor of one third is applied. For integrally stiffened panels or panels with very flexible stiffeners f_r and σ_o are derived from the procedure proposed in section 3.4. Where experimental values of frequency are available these have also been used in the estimates. Thus two theoretical values of r.m.s. stress are given – one based on the measured frequency (if available) and one based on the computed frequency. In some cases use of the experimental frequency presents a difficulty because the response is multimodal in form. The mid frequency of the response band has been used in such cases.

4.1. Flat Plates

The only results available for single plates fully fixed around their edges are those published by N.A.C.A.[11,12]. These are used directly to show that in this case the experimental values are in good agreement with the theoretical results based on equation 34. To get this good agreement, measured values of the predominant frequency and of the damping were used.

16

The more important practical case is that of plates which are flexibly mounted along their edges on frames and stringers to form a built up panel such as a fuselage side. Results for tests on this type of structure are given in table 1 and compared with the single plate results in figure 5. The data used here comes from plates which have a slight curvature as well as from flat plates but it is considered that the effect of curvature (down to about 3 ft radius on 6 in. wide panels) is not very great.

In figures 5 and 6 the experimental values are compared with estimates made from equation 35. In figure 5 the estimated values are based on an experimentally determined value of frequency whilst in figure 6 the theoretical value of frequency is used. Comparison of the two figures shows that there is little difference in the accuracy of the two estimates. This is partly due to the fact that the estimated r.m.s. stress level varies as the square root of the frequency and partly due to the relatively wide bands (factors of 2) which are considered to constitute a reasonable estimate in this process. The one set of measurements which show the greatest difference from the estimates are those relating to stress in the skin directly over the stiffener web and over the edge of the stiffener flange. In this position close to the plate edge fixing the stress is varying rapidly with distance away from the edge. Thus the strain gaugue is integrating the strain over a significant distance and the measured mean value is much less than the true maximum at the edge.

With the exception of this latter set of results, the figures show that the estimated stress levels are within a factor of 2 of the measured values. In view of the very severe simplifications which have been made in the theory this is considered to be good agreement. The reason for this good agreement is thought to be primarily due to two of the major assumptions having opposite effects on the result. If a single plate is being excited by a pressure loading which is in phase over its whole length the stress induced in the plate should be close to that predicted. But if now the plate is connected to other plates around its edges two main effects become important. In the first place the lowest mode of vibration is generally one in which adjacent plates vibrate out of phase. For jet noise loading of typical structures the pressure correlation pattern is such that pressures over several plates in the group are in phase.

17

Thus the generalised force is considerably reduced and the response in that mode is much lower than the single plate case. However, coupling of the plates together introduces extra normal modes which have significant response. We have the situation then in which the response in one of the modes of the built up structure is much lower than the estimated response of a single plate but there are many significant modes whose responses must be added to give the overall r.m.s. stress. The results available to date show that the single plate estimate also gives a reasonable estimate for the built up panel.

4.2. Control Surfaces

More experimental results are available for control surface types of structure as these have been the structural areas where most damage has been sustained in the past. The estimates are obtained from the modified form of equation 35 as described in section 3.3. The actual equations used are:

Excitation on one surface (elevators)

$$\sqrt{\overline{\sigma^2(t)}} = 0.0157 \; S_{PL} \; f_r^{\frac{1}{2}} \; \sigma_o \qquad \qquad ..36.$$

Excitation on both surfaces (rudders - except in one engine tests)

$$\sqrt{\overline{\sigma^2(t)}} = 0.0222 \; S_{PL} \; f_r^{\frac{1}{2}} \; \sigma_o \qquad \qquad ..37.$$

The results available are summarised in Table 2 and the comparison of estimated and experimental r.m.s. stresses is shown in figure 7 and 8. Figure 7 shows the comparison of estimates based on the experimental frequency and figure 8 shows the comparison with estimates based on the theoretical frequency. Both figures 7 and 8 show that the majority of the estimates are within a factor of 2 of the experimental results.

The reasons for this good agreement are similar to those outlined in the discussion in section 4.1. as again the response is generally multi modal in form. In this case however the situation is somewhat more complicated by the different ratios of rib material to skin plating material. Where there is excitation predominantly on one skin some structures have almost equal stresses in the two skins (test series 5 for example) whereas others show differences of the order of a factor of 2 (test series 6). However it seems that the factor of 2 on the estimates is sufficiently large to cover the deviations of the experimental from the theoretical results. There is no significant difference in the agreement achieved with the two types of estimate.   18

4.3. Integrally Stiffened Panels

The test results available on integrally stiffened panels relate to test specimens rather than to complete structures. The two types of structure are described in the Appendix under test series 12 and 13. The first of these two is a multi-bay box structure representing a section out of a full scale fin. The two skins of this box are integrally stiffened and the webs of the ribs and spars are relatively thin with corrugations to provide the necessary stiffness. The three specimens, 12A, 12B and 12C, have different skin-stiffener configurations as indicated in table 3. The box was subjected to noise on one side only.

Test series 13 relates to tests of curved specimens representing a section of an aircraft fuselage. Several similar specimens made up the test series 13A whereas 13B refers to a single specimen. In 13A the skin is chemically etched to provide a double thickness section at the region where the T section stiffener is attached by a double line of rivets. In 13B the skin has a constant thickness but the stiffener of type 13A is used.

Table 3 summarises the principal dimensions of the test sections and gives the theoretical and experimentally determined frequencies of the predominant peaks in the strain spectra of the skin vibration. The first column of theoretical frequencies have been derived on the assumption of a plate fully fixed on rigid stiffeners. In the case of specimens 12A to C this considerably overestimates the frequencies. The specimens 13A and B have relatively stiffer stiffening members and thus the first column estimates are not so much in error although they are higher than the measured frequencies. In the second column of theoretical results the computations have been based on the Rayleigh-Ritz analysis given in section 3.4. The agreement between these results and the experimental values is close and the major trends are reproduced in the theoretical results. The measured spectra show several peaks and thus the values quoted only represent the most significant of the measured frequencies.

Table 4 gives the comparison of the measured and the theoretical r.m.s. stress levels in the skin at the four measurement positions. Again two theoretical results are quoted but both are based on the frequency computed by the Rayleigh-Ritz method as this gives the closest agreement to the measured frequency. The first column of computed stresses uses the simple single plate equation (35 or 36) whereas the second column uses

19

the more detailed analysis based on the Rayleigh-Ritz results. The difference in the values for the skin stress estimated by the two methods is not great. The main difference between the two is that the simple method gives the stress at the edge of the plate as equal to twice the stress at the centre whereas in the Rayleigh-Ritz results the two stresses are very similar in magnitude. The estimates for positions 3 and 4 by the simple method are approximately zero whereas the Rayleigh-Ritz method gives values which are comparable with the experimental results.

For cases 12A and 12B the experimental values for positions 1 and 2 are considerably greater than the estimates although in 12C the agreement is within the factor of 2. In the curved fuselage sections, 13A and 13B, the experimental values for the edge of the plate are very similar to the values at the centre. This is predicted by the Rayleigh-Ritz results and the agreement with the experimental values is again within the factor of 2.

In general it can be seen that the trend of the results for the r.m.s. stress is predicted by the Rayleigh-Ritz method but the absolute magnitude of the estimates is not always within the scatter factor of 2. The estimates for the integrally stiffened panels are further in error than the estimates for the more heavily stiffened fuselage test panels. Further work is needed to consider in detail the application of this relatively simple method to integrally stiffened panels.

5. Jet Noise in Flight

In the early work on the effect of jet noise on aircraft structures it was assumed that the worst loading case occurred at take off when the engines were operating at full thrust and the aircraft was stationary. This assumption was based on the knowledge that the acoustic pressures varied approximately as the fourth power of the relative velocity of the jet stream in the surrounding air. Thus as the aircraft gathered speed on take off and climb the relative jet velocity fell and the acoustic pressures decreased considerably. This was confirmed by some of the early in-flight strain measurements (see Wagner[13] for example) where the strain levels in cruise were about one quarter of the maximum levels at take-off. The cruise levels in this case were probably due to a residual of jet noise plus boundary layer pressure fluctuations.

20

5.1. Acoustic Pressures

In more recent tests of current aircraft designs it has been found that in some configurations strain levels as high as or even higher than the maximum ground running levels can be obtained in flight. Further investigation has shown that these relatively high in-flight levels are due to shock cell noise from the choked jet flows. The phenomena of shock cell noise was first discovered by Powell[15] in tests on model jets at super critical pressure ratios. In these tests an intense discrete frequency sound was emitted by the choked jet and Schlieren pictures showed clearly the sound wave propagating outwards from the jet. Powell postulated that this tone was due to a feedback mechanism in the jet. He suggested that a disturbance initiated at the lip of the jet propagated downstream within the jet flow until meeting the first shock cell. Then the disturbance at the shock cell propagated back upstream in the surrounding air to repeat the disturbance at the lip. Powell derived an expression for the wavelength of the fundamental tone λ as:

$$\lambda = k(P_R - P_C)^{\frac{1}{2}}D \qquad ..38.$$

where

P_R = nozzle pressure ratio

P_C = nozzle critical pressure ratio

D = nozzle diameter

k = constant of value approximately 3

Equation 38 relates to a stationary nozzle but allowance can be made for forward speed of the aircraft by adjusting the time taken by the sound wave to travel in the upstream portion of the feed-back loop. On the assumption that the cell length is unchanged by forward speed the modified expression has been found to give reasonable agreement with measured flight frequencies.

This shock cell instability produces a sound having marked directional characteristics. In a stationary jet the maximum intensity of the fundamental frequency is in a narrow lobe close to the jet axis whereas the lobe for the second frequency is at approximately 90° to the jet axis. These angles are modified in the forward flight case but in practice the second frequency, at twice the value of the fundamental, causes the most significant pressure loading on adjacent structure.

21

Powell's work suggests that the spectrum of noise output of a choked jet would have a smooth broad band component due to the turbulence, as in the case of a subsonic jet, plus spectral lines at the fundamental frequency and at multiples of this. Even in tests on model jets inconsistencies were observed. In some cases the shock cell noise was present as a very narrow band peak in the noise spectrum whereas in other cases the peak was much broader.

In measurements on full scale engines at the time of Powell's model test shock cell noise was not detected. However, current jet engines have considerably higher pressure ratios and the phenomena is now becoming important in full scale jets. A typical spectrum for noise pressures on the undersurface of the tail plane of a rear engined aircraft is shown in figure 9 for different altitudes during a climb to 40,000 ft. In this case the shock cell noise contribution to the spectrum appears as a relatively broad peak whose frequency decreases with increase in pressure ratio as would be predicted by equation 38. The amplitude of the peak increases with increase in pressure ratio but as the phenomenon is essentially due to an instability it has not yet been possible to compute the amplitude from Powell's theory. Corrugated nozzles change the form of the spectrum but do not eliminate the shock cell noise component. Convergent-divergent nozzles can be designed to eliminate shock cells at any one pressure ratio but as the engine will have to operate over a range of pressure ratios this is not the complete answer to the problem.

5.2. Stress Levels

Figure 9 shows that the frequency of the second peak which radiates at 90° to the jet centre line varies from approximately 500 c.p.s.-60 c.p.s. as the pressure ratio of the engine increases during climb. Equation 38 shows that the frequency is inversely proportional to jet diameter and thus for a given variation in pressure ratio the frequency range for a smaller diameter jet would be higher than that shown in figure 9. This frequency range covers a typical range of values of skin plate natural frequencies and thus the peak in the excitation will slowly sweep through the frequency range of the major skin resonances. As a result of this, skin structure in the region of the exit plane of the nozzle will show high stresses at a point in the climb or cruise if the excitation peak corresponds to a plate resonance. Figure 10 shows a typical variation

22

of short term r.m.s. stress level in a rudder skin panel during take off
and climb for a different aircraft from the one to which figure 9 refers.
The r.m.s. values quoted are measured from 10 second samples of the
continuous record. As would be expected, the relatively high initial
level at brake release falls rapidly as the aircraft gathers speed along
the runway. The stress level then slowly increases as the aircraft climbs
and a stress maximum is reached at about 23,000 ft. in this particular
structure on this civil airliner. Measurements on other parts of the
structure having different natural frequencies show peaks occurring at
different positions in the flight profile.

Further illustration of this effect is shown in figure 11 where
the strain spectrum at take off is compared with the spectrum in one of the
flight cases. It can be seen that the broad band excitation at take off
excites several modes of vibration in the frequency range 160 to 320 c.p.s.
The flight spectrum, however, shows that the mode at 280 c.p.s. has been
accentuated in amplitude whereas the others at either side in frequency have
been attenuated. This is a good example of the effect of narrow band
excitation.

In this particular case the stress levels are too low to cause
any fatigue failure but in another type of aircraft fatigue failures due to
shock cell noise did occur. The main consideration from the fatigue point
of view is that the relatively high stresses can be present during a much
longer portion of a typical flight than was the case when only ground noise
was important.

6. Fatigue Aspects

In cases of jet noise excitation, the stress levels are
generally low by structural standards but because of the high frequency
a large number of stress reversals occurs in the life of an aircraft.
Schelderup[16] has shown that in practical cases the stress has a
Rayleigh distribution for peak to trough values. This suggests that
fatigue test data obtained with this type of distribution should be
applicable to the acoustic fatigue case. All that is required now is
to have random S-N curves obtained with a Rayleigh distribution of stress
and having the r.m.s. stress and the number of reversals as the ordinates.
The number of reversals can be obtained from the number of zero crossings
of a random wave form as discussed by Clarkson[17]. A typical curve

23

obtained this way is shown in figure 12 which has been taken from the
Royal Aeronautical Society Data Sheets on Fatigue[18].

The suggested design procedure is to use the methods outlined
above to obtain an estimate of the r.m.s. stress and then to use the
random S-N curves to obtain an estimate of life. Knowing the likely
inaccuracies in the stress estimates, the individual designer must choose
what safety factor he is prepared to use.

7. Conclusions

The results quoted in this report show that in a relatively
wide range of typical aircraft structures the overall r.m.s. stresses
induced by jet noise can be estimated by a development of the simple
relationship due to Miles. The estimated stresses are generally within
a factor of 2 of the measured values. In view of the likely inaccuracies in
the noise measurements and in the severe simplifications in the theory this
order of agreement is considered to be satisfactory. The many possible
reasons for the discrepancies have been indicated in the discussion of the
test results. A greater accuracy would require a much more complicated
multi-modal analysis of the structural response. These results show the
order of accuracy which should be achieved with simple design procedures
such as that proposed in the Royal Aeronautical Society Data Sheets on
Acoustic Fatigue and the Douglas design charts. The simple procedure
suggested for application to integrally stiffened panels gives a good
agreement on frequency of predominant modes of vibration but less good
agreement on stresses. As the bending stiffness of the integral stiffener
relative to the plate is increased the accuracy of stress prediction
increases towards the factor of two achieved in the conventional built-up
structure. More work is required on integrally stiffened skins.

REFERENCES

1. Clarkson, B.L.
   Ford, R.D.
   "The Response of a Typical Aircraft
   Structure to Jet Noise"
   Journal Royal Aeronautical Society
   January 1962.

2. Clarkson, B.L.
   Ford, R.D.
   "Random Excitation of a Tailplane
   Section by Jet Noise"
   ASD TDR-62-680.

3. Schjelderup, H.C.
   "Structural Acoustic Proof Testing"
   Aircraft Engineering, October 1959.

4. Powell, A.
   "On the Fatigue Failure of Structures
   Due to Vibrations Excited by Random
   Pressure Fields"
   J.A.S.A. Vol. 30. Dec. 1958.

5. McGowan, P.R.
   Frasca, R.L.
   "Structural Design for Acoustic Fatigue"
   ASD TR-63-820.

6. Robson, J.D.
   "An Introduction to Random Vibration"
   Edinburgh University Press 1963.

7. Mercer, C.A.
   "Response of a Multi-supported Beam to
   a Random Pressure Field"
   J. Sound & Vibration Vol. 2 p.293 (1965).

8. Miles, J.W.
   "On Structural Fatigue under Random
   Loading"
   J. Aero. Sc. Vol. 21 p. 753-762 (1954).

9. Timoshenko, S.P.
   Woinowsky-Krieger, S.
   "Theory of Plates and Shells"
   McGraw-Hill. 2nd Edition 1959.

10. Lin, Y.K.
    "Free Vibrations of Continuous Skin
    Stringer Panels"
    J. Applied Mechanics, Dec. 1960.

11. Lassiter, L.W.
    Hess, R.W.
    Hubbard, H.H.
    "An Experimental Study of the Response
    of Simple Panels to Intense Acoustic
    Loading"
    J. Aero. Sciences Vol. 24 p.19 (1957).

12. Lassiter, L.W.
    Hess, R.W.
    "Calculated and Measured Stresses in
    Simple Panels Subject to Intense
    Random Acoustic Loading Including the
    Near Noise Field of a Turbojet Engine"
    N.A.C.A. T.N.4076 (1957)

13. Wagner, J.C.
    "Caravelle Acoustical Fatigue"
    I.C.A.F.-A.G.A.R.D. Symposium, Paris
    May 1961.

14. Lin, Y.K.   "Stresses in Continuous Skin-Stiffener
                                      Panels under Random Loading"
                                      J. Aerospace Sciences Vol. 29 p. 67(1962).

15. Powell, A.   "On the Mechanism of Choked Jet Noise"
                                      Proc. Phys. Soc. Vol. 66B(1953).

16. Schjelderup, H.C.   "Aspects of the Response of Structures
    Galef, A.E.   Subject to Sonic Fatigue"
                                      ASD TR 61-187.

17. Clarkson, B.L.   "The Design of Structures to Resist Jet
                                      Noise Fatigue"
                                      J. Royal Aero. Soc. Vol. 66 p. 603(1962)

18. Royal Aeronautical Society   "Data Sheets on Fatigue"
                                      No. 66022 (1966)

TABLE 1   R.M.S. STRESS IN FLAT AND SLIGHTLY CURVED PANELS

Test	Gauge Pos.	Plate Dimensions					Frequency c/s		Noise Level dB		Stress r.m.s. lb./in.²		
		R in.	b in.	t in.	a/b	σ_0	Theory f_0	Exp. f_1	OA	Spect.	Est.:f_0	Est.:f_1	Exp.
2A	C	38	2.75	0.047	2.4	850	1,430	600	150	120	618	400	578
	C	38	3.40	"	1.9	1,290	970	725	"	"	775	570	1,090
	C	"	3.62	"	1.8	1,440	880	725	"	"	825	750	919
	C	"	4.44	"	1.5	2,020	610	600	"	"	960	955	868 } 651
	C	"	3.65	"	1.8	1,460	590				830	685	820
	C	"	5.46	"	1.2	2,570	460	570	"	"	1,060	1,180	1,015
	C	"	3.46	"	1.9	1,330	700	725	"	"	680	690	868
	C	"	4.64	"	1.4	2,100	550	605	"	"	955	1,000	515
2B	2	"	3.62	"	1.8	2,880	880	725	"	"	1,650	1,500	257
	1	"	4.44	"	1.5	4,040	610	725	"	"	1,930	2,100	789
	2	"	4.44	"	1.5	4,040	610	725	"	"	1,930	2,100	820
	1	"	3.65	"	1.8	2,880	860	590	"	"	1,630	1,350	515
3	C	∞	7.35	0.040	≈1	5,200	256	355	149	116	1,010	1,200	1,250 } 1,500 } 860 } 950 }
4	E	∞	8.2	0.040	>2	20,900	136	100 } 300 }		119 125	6,630	8,050	4,000 } 8,000 }

27

TABLE 2 R.M.S. STRESS IN CONTROL SURFACE SKIN PLATES

Test	Gauge Pos.	Plate Dimensions b in.	t in.	a/b	σ_0	Frequency c/s Theory f_0	Exp. f_1	Noise Level dB OA	Spect.	Stress r.m.s. lb./in.² Est.:f_0	Est.:f_1	Exp.
5R	C	4.125	0.05	4.5	1,700	750	450	150	122	535	415	1,290 1,090
	C	3.75	0.04	4.5	2,200	775	450	148	121	613	475	950 945
	E	3.75	0.04	4.5	4,400	775	450	148	121	1,230	950	1,230 1,070
	E	4.125	0.05	4.5	3,400	750	450	150	121	950	734	1,780 1,340
	E	"	"	4.5	3,400	750	450	150	121	950	734	2,560 1,220
5E	1	4.0	0.05	4	3,200	705	560	152.5	123	770	687	1,470 1,190
	2	4.0	0.05	4	"	705	600	"	"	770	712	845 600
6	E	6.86	0.052	1.04	14,900	220	150	155	122	1,800	1,490	846
	E	5	0.025	2.1	20,000	230	300	"	123.5	2,950	3,360	1,763
	E	4.1	0.032	>2	8,200	380	400	"	125	1,850	1,900	1,340
	C_u	"	"	"	4,100	380	420	"	125	920	975	2,630
	E_u	"	"	"	8,200	380	420	"	"	1,850	1,950	1,100
	C_ℓ	"	"	"	4,100	380	300	"	"	920	823	4,040
	E_ℓ	"	"	"	8,200	380	340	"	"	1,850	1,750	2,250
7	E	6	0.063	>2	4,550	394	500	162	134	2,960	3,340	2,600
	C	"	0.063	"	2,275	"	"	161	133.5	1,410	1,590	1,570
	E	"	"	"	4,550	"	"	161	133	2,610	2,940	2,500
	C	"	"	"	2,275	"	"	160	132.5	1,230	1,390	1,500
	E	"	"	"	4,550	"	"	160	132	2,320	2,620	1,770
	E	"	"	"	"	"	"	157	127	1,290	1,460	1,300
	C	"	"	"	2,275	"	"	157	127	650	730	1,000
	C	"	"	"	"	"	"	155	126	580	650	770
	E	"	"	"	4,550	"	"	155	126	1,150	1,300	830
8	E	6	0.02	>2	45,000	125		137	112	1,300		450
	E	"	0.02	"	"	"		"	"	1,300		390
	E	"	0.045	"	8,850	281		140	113	430		220 280
	E	"	0.045	"	"	"		"	"	"		310

TABLE 2 (continued) R.M.S. STRESS IN CONTROL SURFACE SKIN PLATES

Test	Gauge Pos.	Plate Dimensions				Frequency c/s		Noise Level dB		Stress r.m.s. lb./in.²			
		b in.	t in.	a/b	σ_o	Theory f_o	Exp. f_1	OA	Spect.	Est.:f_o	Est.:f_1	Exp.	
8	E	5.75	0.04	>2	10,300	272		139	112	440		450	350
	E	"	"	"	"	"		"	"	"		620	700
	E	"	"	"	"	"		"	"	"		390	490
9	C	6.15	0.048	2.7	4,100	286	380	148.5	118	390	450	1,075	
	C	"	"	"	"	"	"	"	"	"	"	687	
	C	6.5		2.5	4,600	254	"	"	"	413	506	1,250	
10R	C	4	0.036	>2	3,080	500	400	150.5	118.5	370	330	670	526
	E	"	"	"	6,160	500	400	"	"	740	660	662	
	C	6	"	"	6,920	225	250	149	115.5	406	428	745	581
	E	"	"	"	13,840	225	250	"	"	812	856	796	
10E	C	6	"	"	6,920	"	350	149.5	117	471	588	788	454
	E	"	"	"	13,840	"	600	"	"	940	1,540	334	
11R	C	6.1	0.028	>2	11,900	170	230	151	116.5	650	760	1,030	1,130
	E	"	"	"	23,800	170	230	"	"	1,310	1,520	1,100	
11E	C	"	"	"	11,900	170	200	152.5	118	770	840	1,570	1,320
	E	"	"	"	23,800	170	210	152.5	118	1,550	1,720	1,140	
	E	"	"	"	"	170	210	154	119.5	1,930	2,150	1,930	

29

TABLE 3   FREQUENCY OF FUNDAMENTAL MODE OF INTEGRALLY OR WEAKLY
STIFFENED PANELS

Test Series		Panel Dimensions in. units				Frequency*		
		b	t	a/b	I	F.F.	R-R	Exp.
12	A	2.57	0.07	5.8	0.0049	2,330	422	225) 375 } 525)
	B	3.0	0.065	5.0	0.0059	1,590	432	412) 475 } 575)
	C	2.5	0.083	6.0	0.0146	2,920	688	550 } 650)
13	A	3.8	0.036	5.3	0.0162	550	372	260) 360 } 900)
	B	4.3	0.064	4.6	0.0162	760	317	250 } 350)

* F.F.   Computed on assumption of single plate fully fixed
at stiffeners

R-R   Computed from the Rayleigh-Ritz Method outlined in
Section 3.4 (Equation 27)

TABLE 4   COMPARISON OF ESTIMATED AND MEASURED STRESSES IN
INTEGRALLY STIFFENED PANELS

Test Series	Pos.	σ_o Eqn. 35 or 36	σ_o Eqn. 30-33	S_{PL} dB	r.m.s. Stress lb./in.^{2} Eqn. 35 or 36	Eqn. 30-33	Exp.
12 A	1	337	433	128	114	147	400 to 900
	2	674	290		228	98	
	4	~0	2370		~0	800	700 to 750
12 B	1	530	640	128	180	220	580 to 840
	2	1060	507		360	170	
	3	0	230		0	80	700
	4	~0	2260		~0	780	
12 C	1	226	400	124	60	107	170 to 200
	2	452	340		120	91	110 to 130
	3	0	100		0	27	
	4	~0	1280		~0	340	110 to 170
13 A	1	2770	3580	128	2640	3420	1400 to 1850 ⎫ 1300 to 2030 ⎬ 1270 to 1640 ⎭
	2	5540	3480		5280	3320	1430 to 2600 ⎫ 1370 to 1800 ⎬ 1350 to 2100 ⎭
13 B	1	1130	1280	127	870	990	440 to 510
	2	2260	1160		1740	890	440 to 580

31

APPENDIX

Structural Details and Test Information

Test Series No. 1

Single flat plates with fully fixed edges

Dimensions 11" x 13" overall

9⅜" x 11⅜" between edge supports

Thickness 0.032, 0.040 and 0.064 in.

Measured frequencies: for $t = 0.040$ $f = 148$ c.p.s.

Overall Sound Pressure Levels:

4 in. diam. cold air jet	:	125 to 135 dB
Jet engine	:	135 to 145 dB
Jet engine plus afterburner	:	146 to 155 dB

Note: Experimental and computed results using Miles formula (equation 34) are given in references 11 and 12. These are plotted directly in figure 5 as the theoretical results are based on measured frequencies.

As this report is primarily concerned with built up structures these single plate results are not quoted in detail.

Test Series No.2

Caravelle Rear Fuselage Skin

References 1 and 13 and unpublished test results

Stiffened skin design as shown in the sketch

Dimensions as in Table 1

Test results 2A relate to stress at the centre of the plates and results 2B relate to stress at the stiffener

The response spectrum is broad band in character and thus the frequencies quoted relate to predominant peaks in the spectrum.

Noise pressure information was obtained from separate noise survey carried out with microphones mounted 2 in. away from the surface of the structure.

Gauge Positions
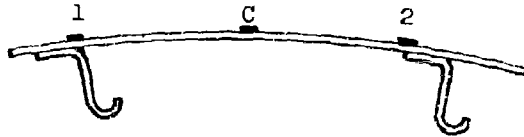
Stringer
Details
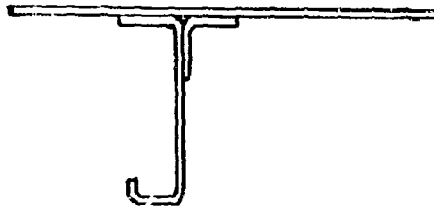
Frame
Details

Test Series No. 3

Caravelle Stub Fin.   Unpublished test results.
Flat skin stiffened with open section members as shown below:

Gauges positioned in the centre of the plates.
Noise pressures obtained as in test series 2.

Test Series No. 4

Rear Fuselage skin panels of Boeing KC135 as reported
in references 10 and 14.

Structural details are as shown in the sketch.
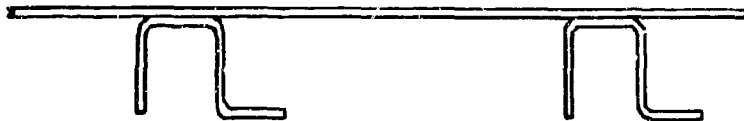
The noise pressure spectrum levels at the two major response
frequencies are given in reference 14. In the estimation procedure the
mean value of these (on a linear scale) has been used and the mean
experimental frequency of 200 c.p.s. This mean value of frequency is
quite artificial as the response spectra shows two very pronounced peaks
having similar magnitudes. Nevertheless the mean value is chosen in
order to be consistent throughout.

Test Series No. 5

Douglas RB66 Rudder and Elevator. Reference 3

The cross section of the rudder and elevator are shown below:

2 1   C   Gauge Positions
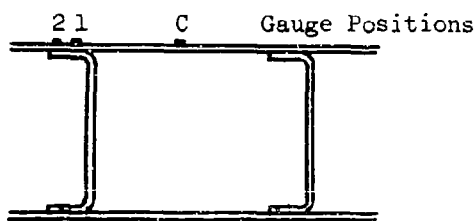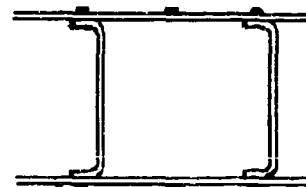
Elevator   Rudder

The noise measurements are only available as octave band levels.

In the elevator measurements two strain gauges were placed on the skin above the joint with the rib. One pair of gauges were directly opposite the web of the rib (marked as position 1) and the other pair were across the edge of the rib flange (position 2). These results are quoted separately as in such situations the strain over the rib web is usually greater than that over the edge of the flange. In table 2 the higher of the two results quoted for position 1 and also for position 2 refer to the bottom skin. The overall noise level on the bottom skin was 152.5dB whereas that on the top skin was only 142 dB. The results quoted for the rudder refer to the response to both engines running. Tests showed that with only one engine operating the stresses were reduced by 3dB as has been assumed in section 3.3. As the response spectra generally have several peaks, the mean frequency has been used in the computation.

Test Series No. 6

Tailplane of small rear engined executive jet aircraft.
Unpublished data.
The structure is as shown in the sketch below and measurements relate to the skin panels.
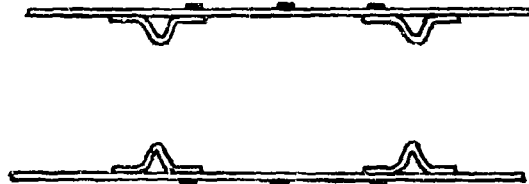
Noise pressure levels were taken from a separate noise survey.

In this test there is a significant difference between the stresses in the upper and lower skin panels. Thus the upper surface panel results are given a suffix u and the lower surface results have a suffix ℓ.

Test Series No. 7

Leading edge of tailplane of a small military aircraft.
Unpublished data.
The structural configuration is as shown below:

35

Gauges Measuring Strain in Spanwise Direction

A comprehensive noise pressure survey was made over the lower surface of
the tail unit.

The stress levels quoted were only peak levels defined as the
largest zero to peak level seen on a 30 second sample. These levels will
be approximately three times the true r.m.s. level. The measured values
have therefore been divided by a factor of 3 to obtain the value quoted in
table 2.

The calculated frequency is based on the assumption of a flat
plate fully fixed at its edges. In this case, although the section of
leading edge skin carrying the strain gauges is approximately flat, it is
a part of a continuous curve forming the leading edge profile. As a result
of this curvature the experimental frequencies are higher than the
predicted values.

Test Series No. 8

Control surfaces of a large military transport aircraft.

Unpublished data.

The details of the structure are shown in the sketch but in this
case the units are a considerable distance away from the engines.
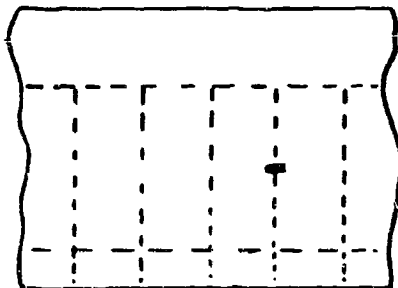
Honeycombe trailing edge

36

The noise pressure levels are relatively low and thus the stress levels are also very low.

Test Series No. 9

Comet tailplane test section.   Reference 2.
A sketch of the structure is shown below.
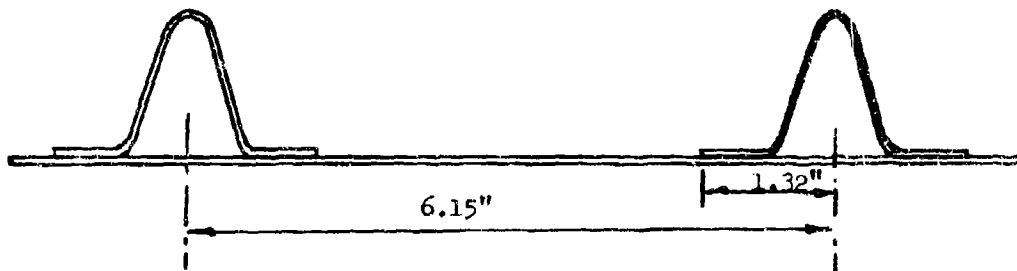
In this structure relatively large closed section stiffeners are used and the flanges of these are of similar dimensions to the width of skin plating between stiffeners.   Although it seems very unrealistic, the full width of plate between stiffener centre lines was used in the estimation procedure.   A more satisfactory method of analysis in such cases is required.

Noise measurements were made using microphones positioned about 2 in. away from the surface of the structure.

Skin response spectra show only one major peak.

Test Series No. 10

Control surfaces of medium sized rear engined civil airliner.
Unpublished data.
Conventional structure as shown in the sketch.
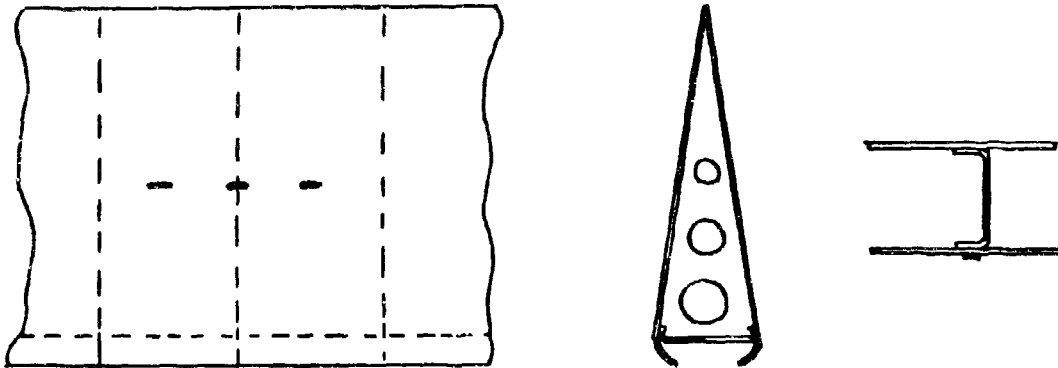
Noise pressures were measured by microphones mounted about 2 in. from the surface of the skin in the ground tests. Flush mounted microphones in the fin and tailplane were used in the flight tests.

The response spectra show several peaks and thus a mean value is quoted in table 2.

Flight test data quoted in section 5 was obtained on this aircraft.

Test Series No. 11

Control surface of a small rear engined executive twin jet aircraft. Unpublished data.
Conventional structure similar in design to that shown for Test Series No. 12. Dimensions different as shown in table 2.

Noise pressure levels obtained from surface mounted microphones.

The response spectra show several peaks and thus the mean value is quoted in table 2. In flight stress response data was also obtained on this aircraft.

Test Series No. 12

Test section of fin having integrally stiffened skin.
Unpublished data.
General layout as shown below:
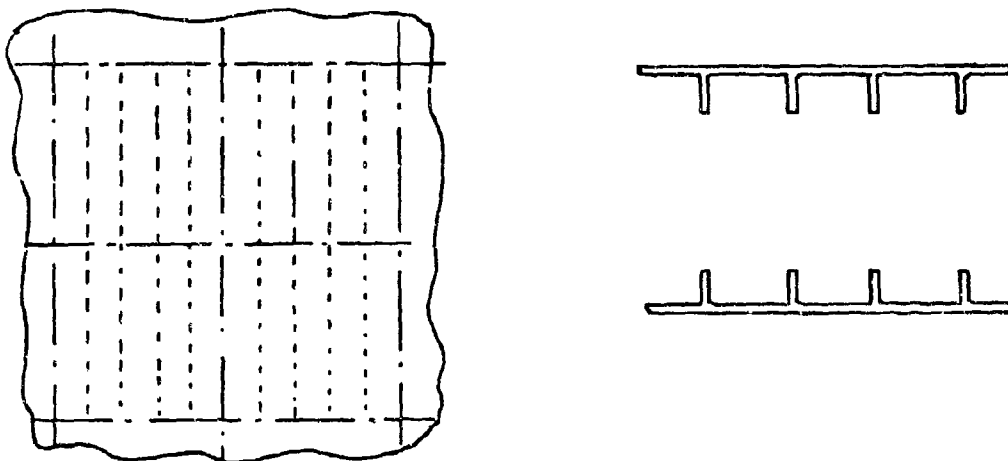
Stiffened skin dimensions are given in table 3. Test section was mounted behind a jet engine. Noise pressure levels obtained from an array of microphones and analysed into one third octave band levels. Strain measurements analysed with a five percent bandwidth analyser. Prior to broad band pressure excitation a discrete frequency excitation was performed in the laboratory to investigate the predominant modes of vibration and their associated damping.

Test Series No. 13

Test section of a curved fuselage having T section stiffeners.

Unpublished data.

Generaly layout as shown below:
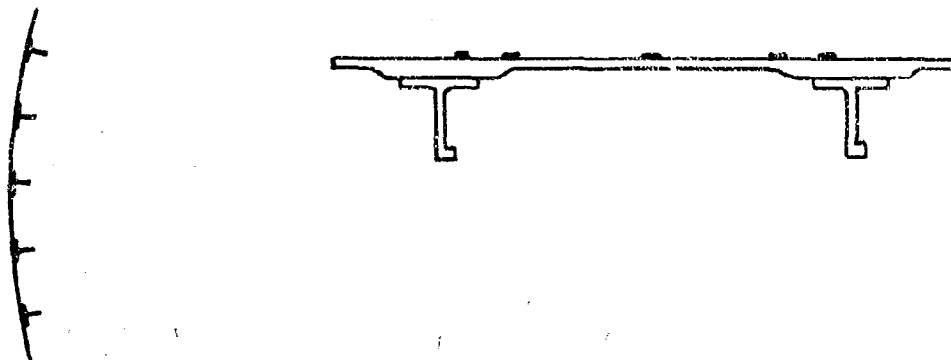
In sore of the test sections chemically etched skin panels were used. In other cases a constant thickness skin was used.

The test procedure was the same as that outlined for test series No. 12.
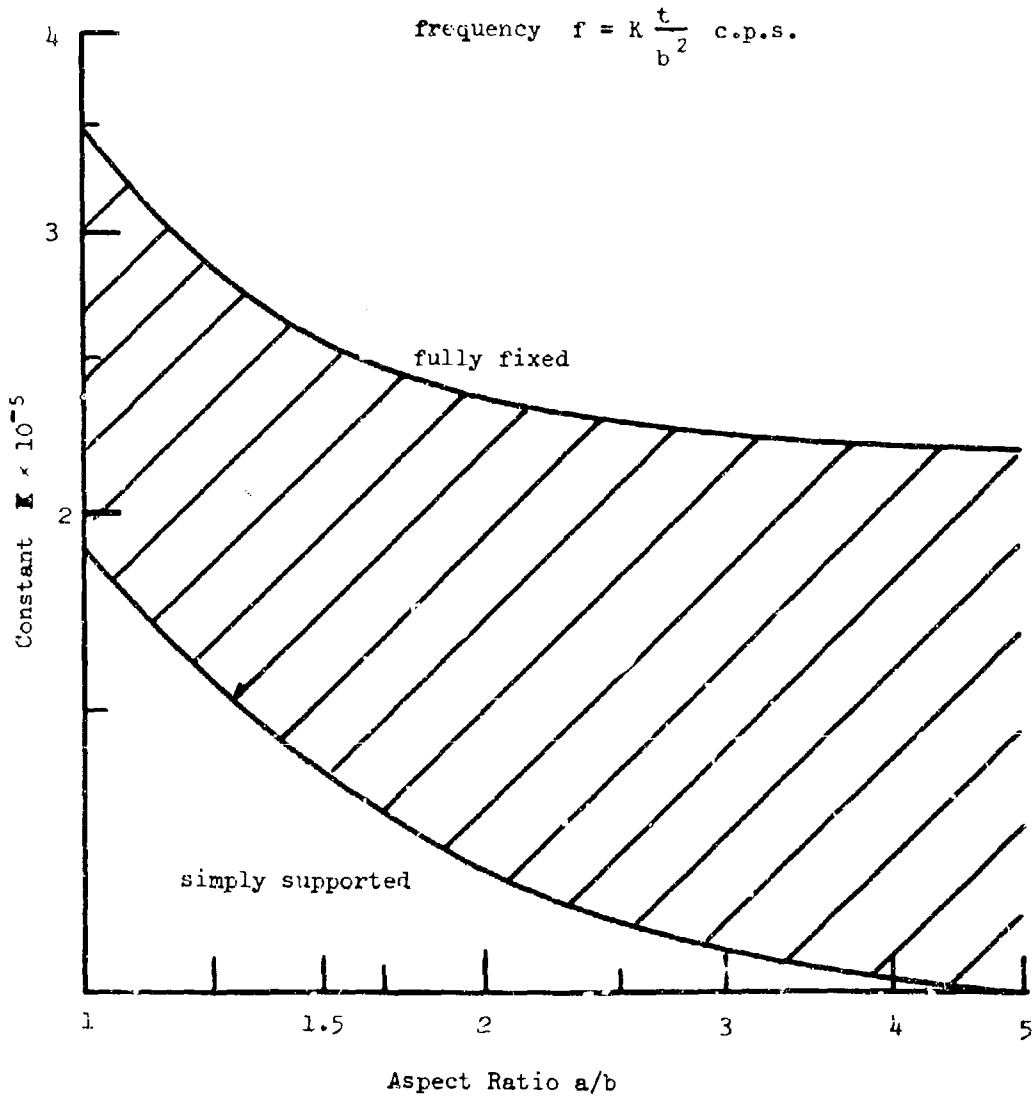
FIG. 1   NATURAL FREQUENCY OF FUNDAMENTAL MODE OF FLAT PLATE

41

Asymptotic Value a/b > 2

$$\sigma_0 = k \ \frac{b^2}{t^2} \quad \text{at fixed edges}$$

$$= \frac{k}{2} \ \frac{b^2}{t^2} \quad \text{at centre}$$
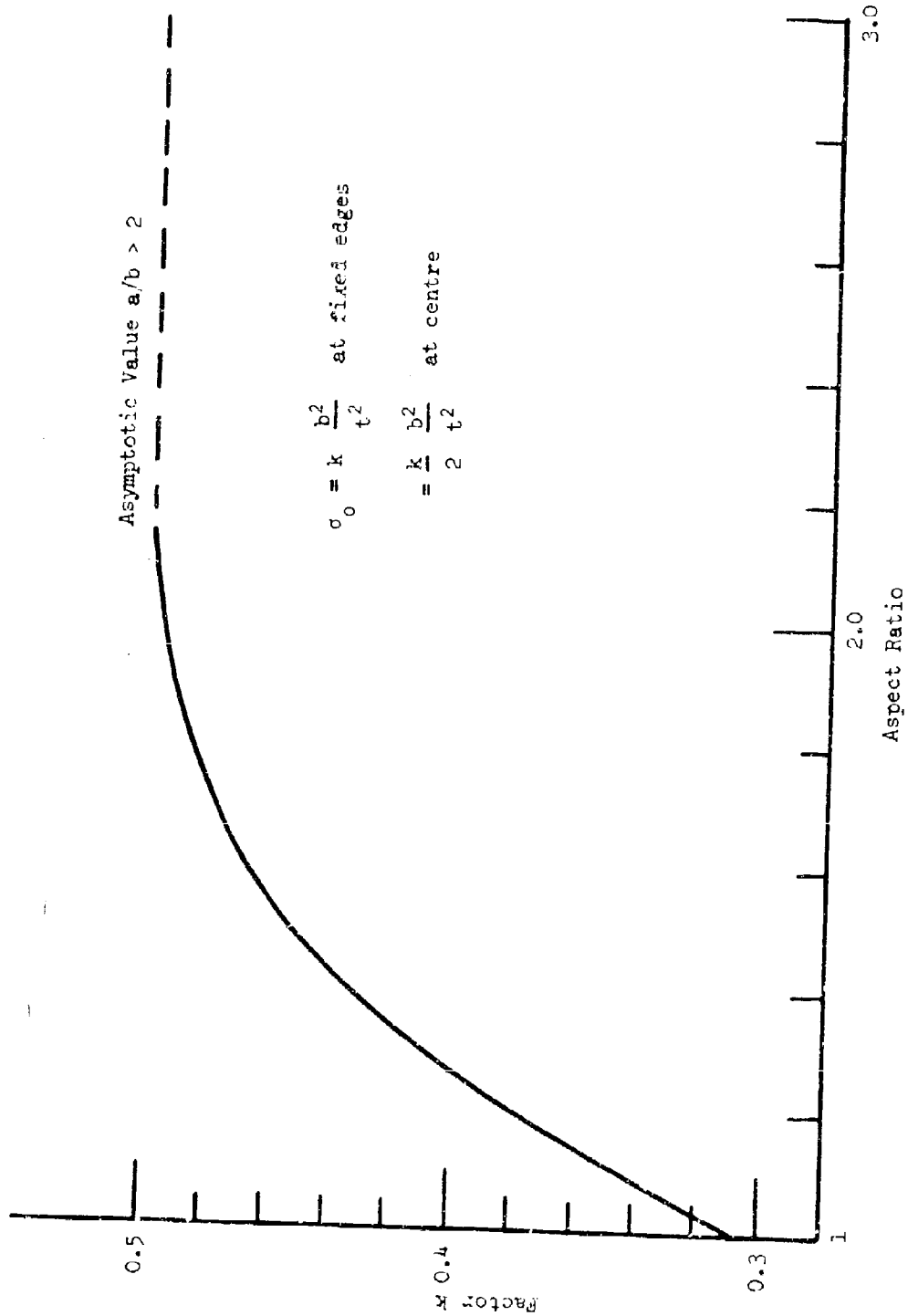
FIG. 2   DETERMINATION OF STRESS PARAMETER σ_0 FOR FLAT PLATES
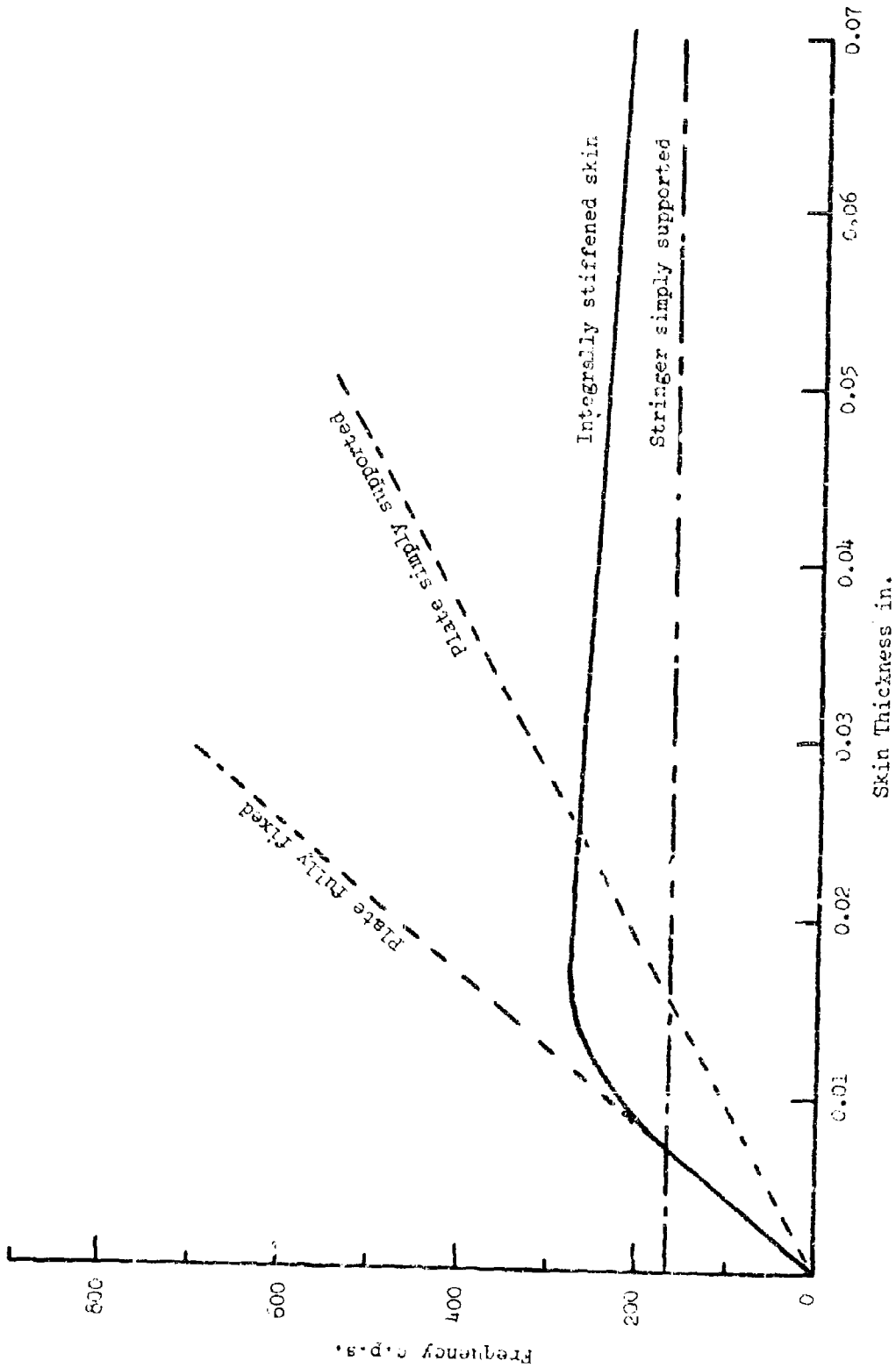
FIG. 3 VARIATION IN FIRST NATURAL FREQUENCY OF AN INTEGRALLY STIFFEND SKIN

43
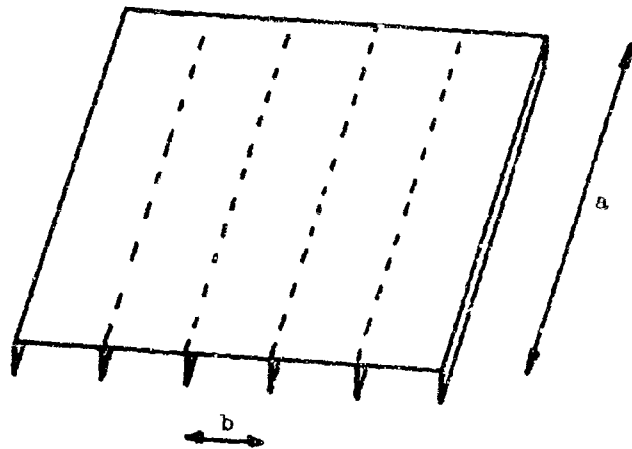
FIG. 4(a)
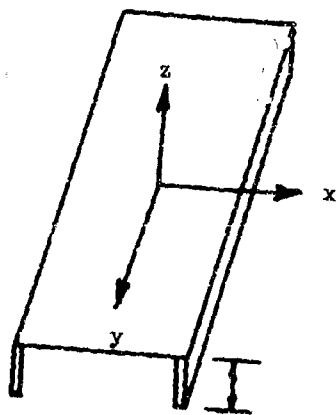
FIG. 4(b)

t = plate thickness

$$D = \frac{Et^3}{12(1-\nu^2)}$$

FIG. 4   INTEGRALLY STIFFENED PANELS

44
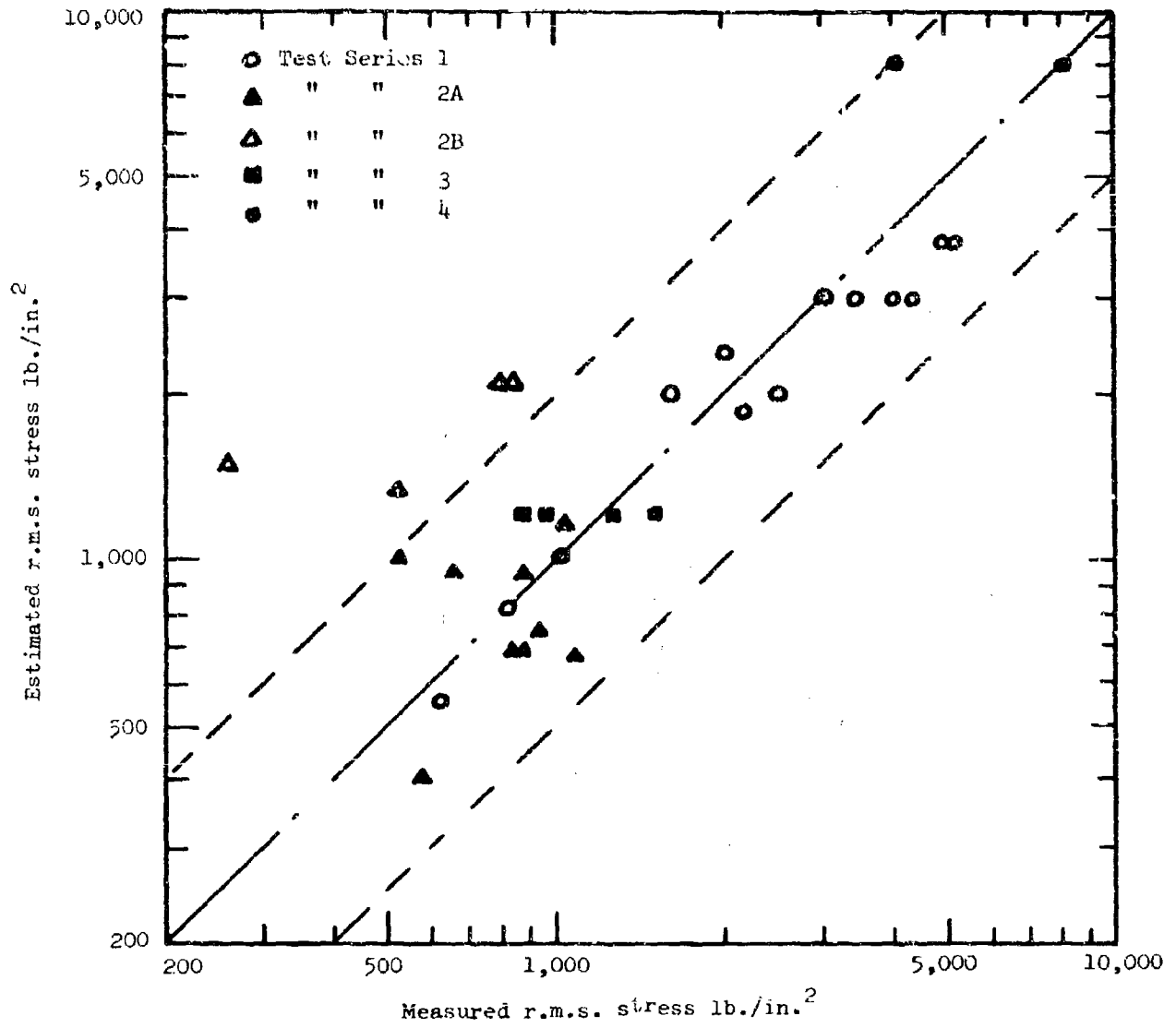
FIG. 5   COMPARISON OF ESTIMATED AND MEASURED R.M.S. STRESS.   FLAT
AND SLIGHTLY CURVED PANELS.   (BASED ON MEASURED FREQUENCY)
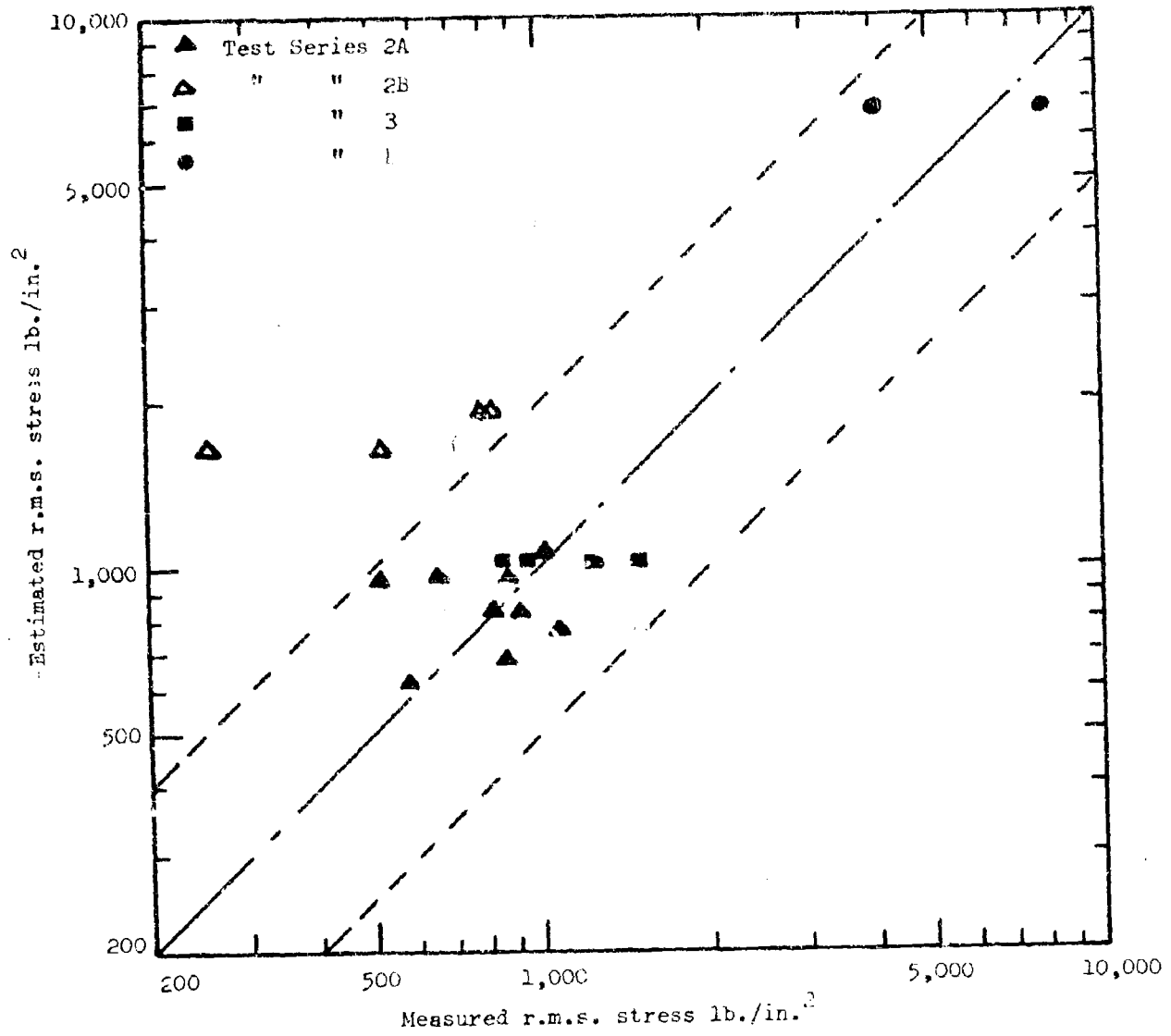
FIG. 6   COMPARISON OF ESTIMATED AND MEASURED R.M.S. STRESS.   FLAT
AND SLIGHTLY CURVED PANELS.   (BASED ON ESTIMATED FREQUENCY)

46
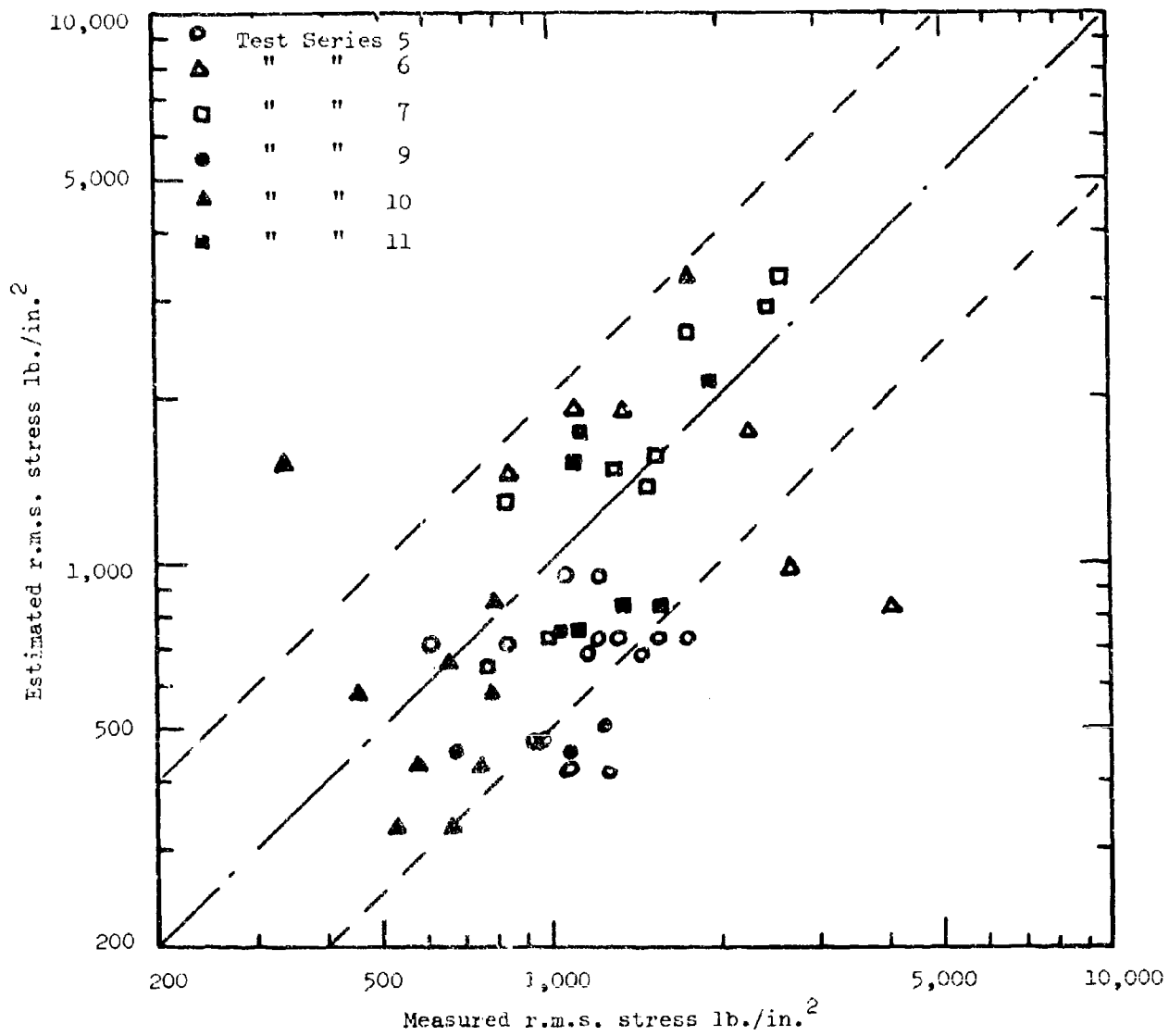
FIG. 7   COMPARISON OF ESTIMATED AND MEASURED R.M.S. STRESS.
CONTROL SURFACES. (BASED ON MEASURED FREQUENCY)
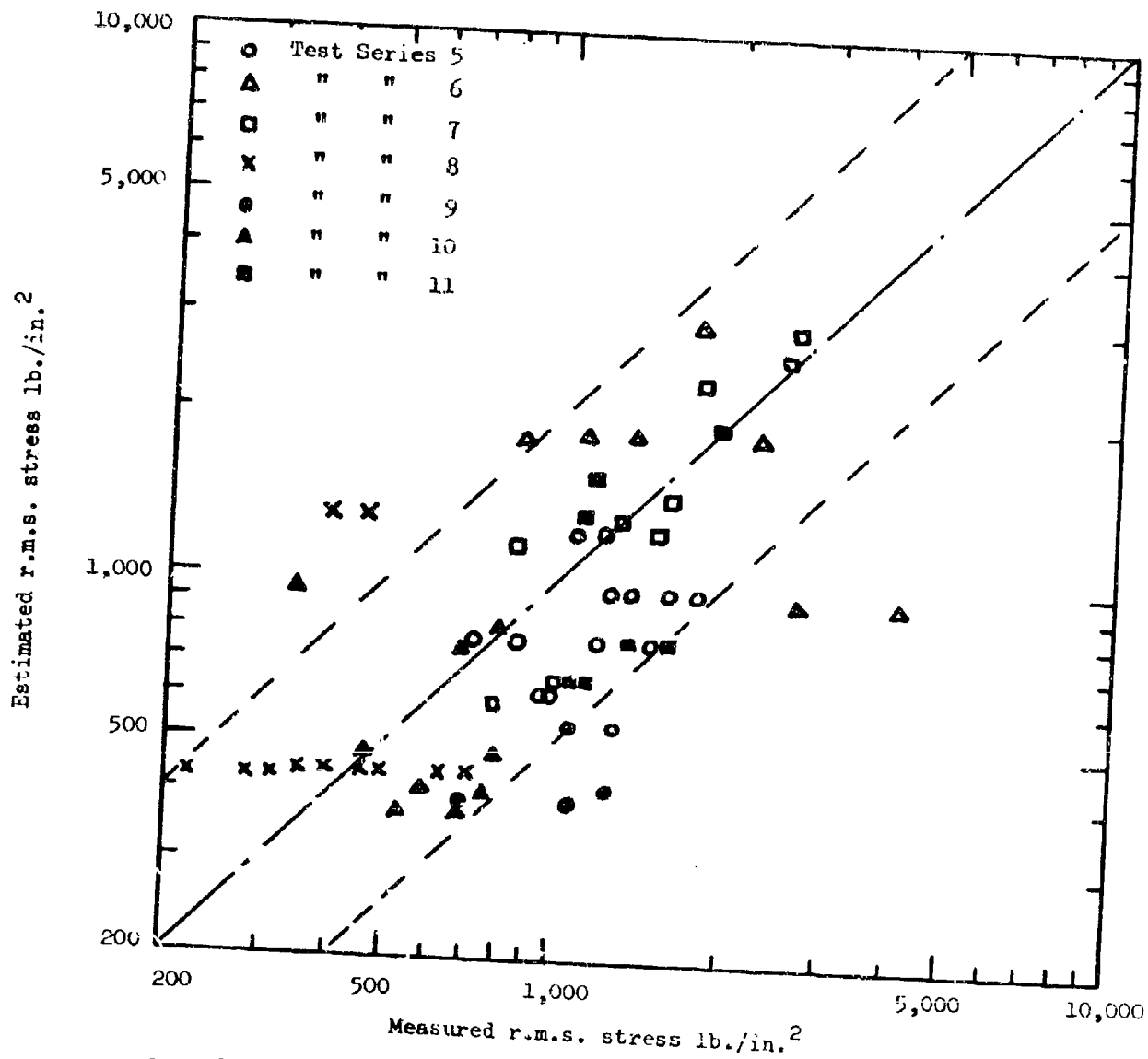
FIG. 8   COMPARISON OF ESTIMATED AND MEASURED R.M.S. STRESS.
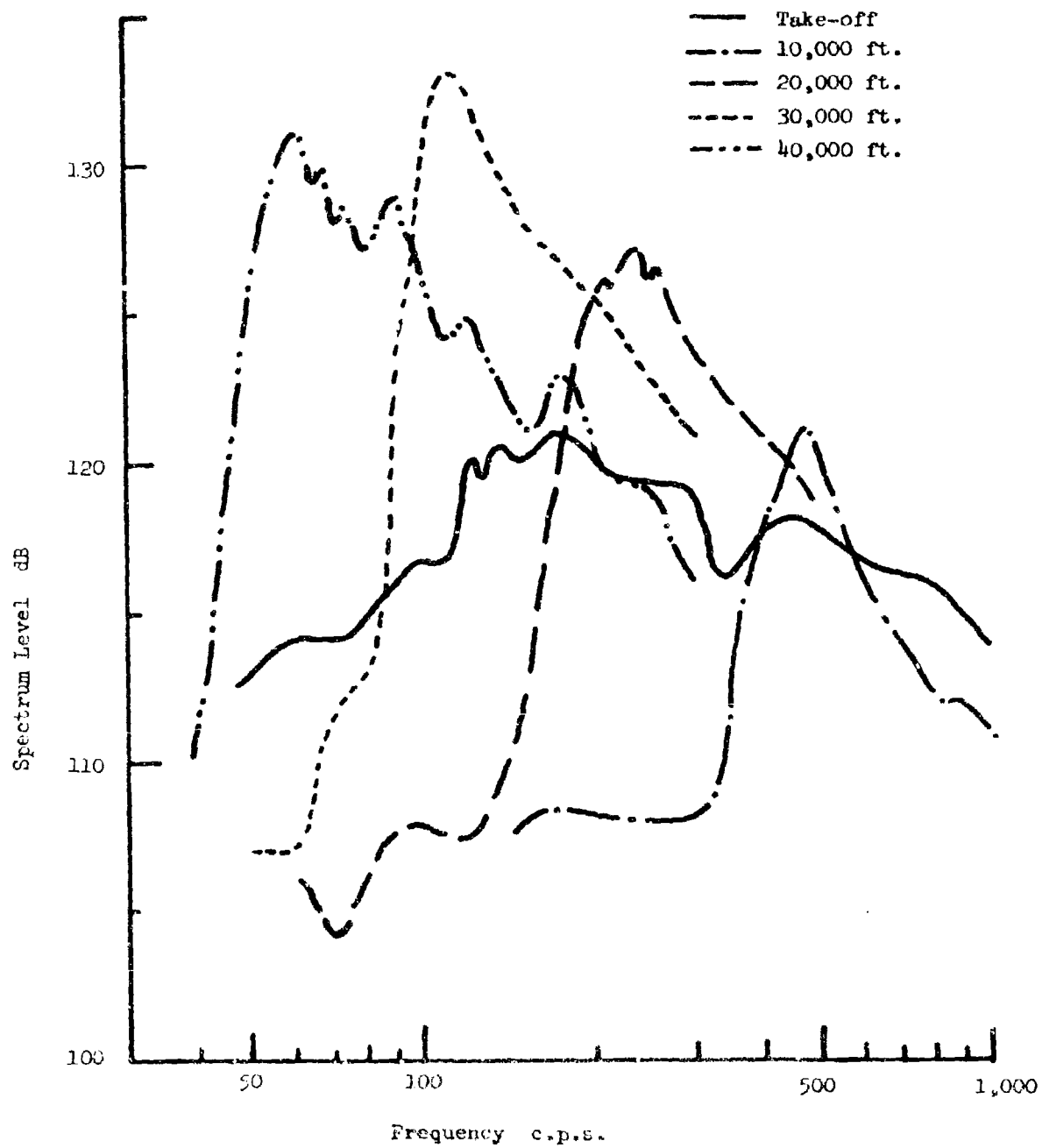CONTROL SURFACES. (BASED ON ESTIMATED FREQUENCY)

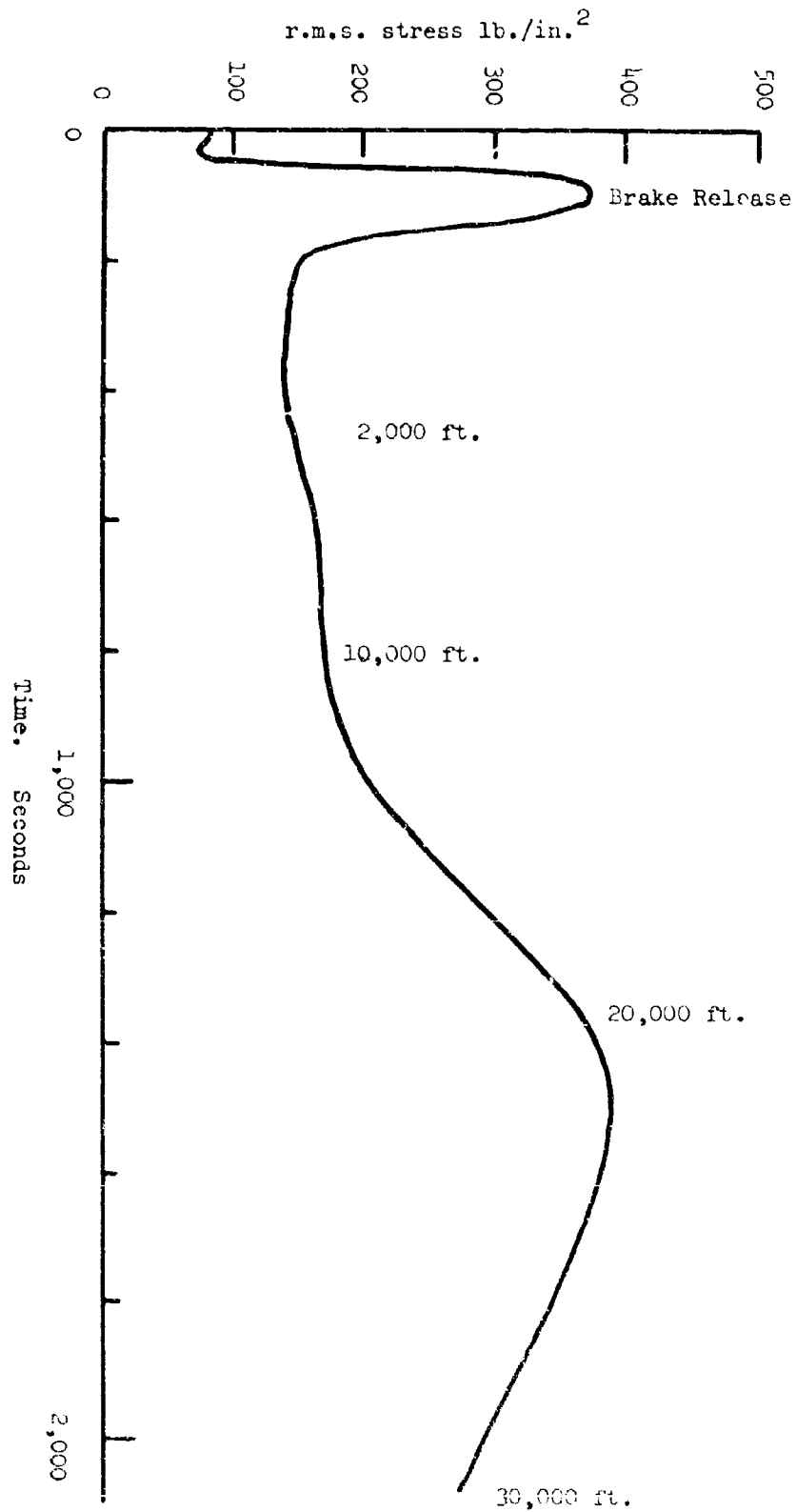FIG. 9 SPECTRUM OF PRESSURES ON TAIL UNIT SURFACE DURING CLIMB

49

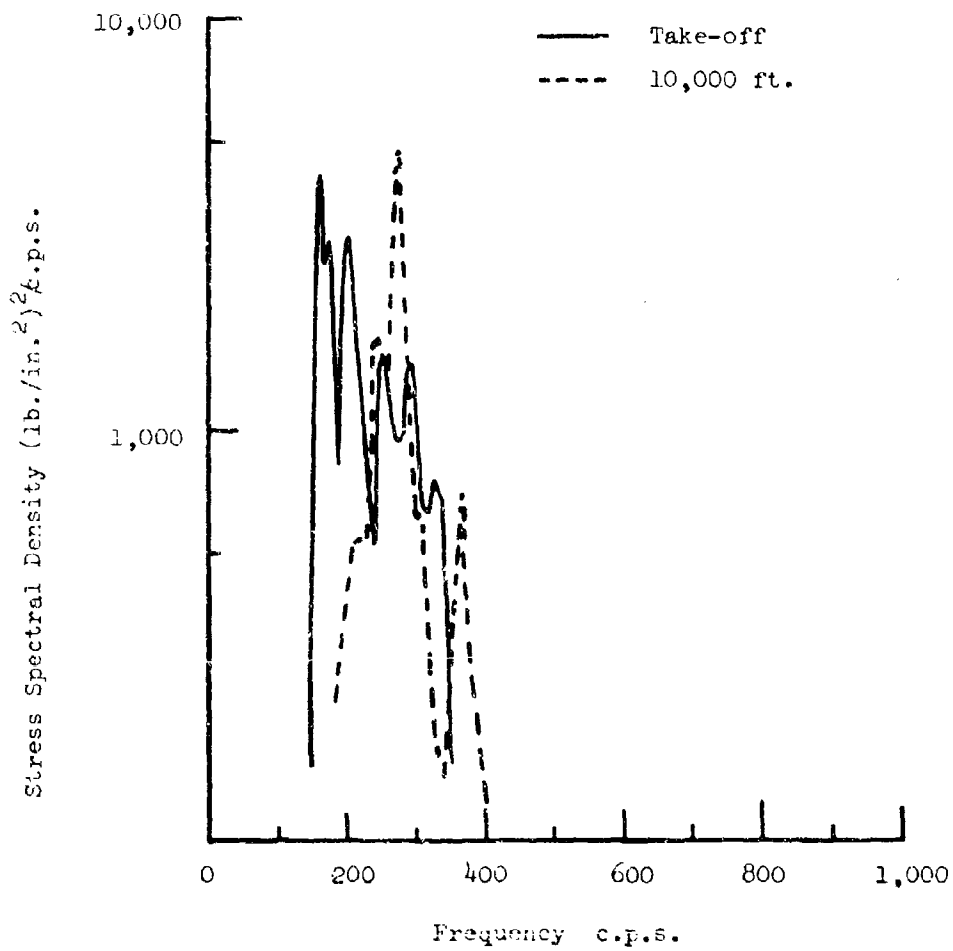FIG. 10 VARIATION IN RUDDER SKIN STRESS DURING TAKE-OFF AND CLIMB

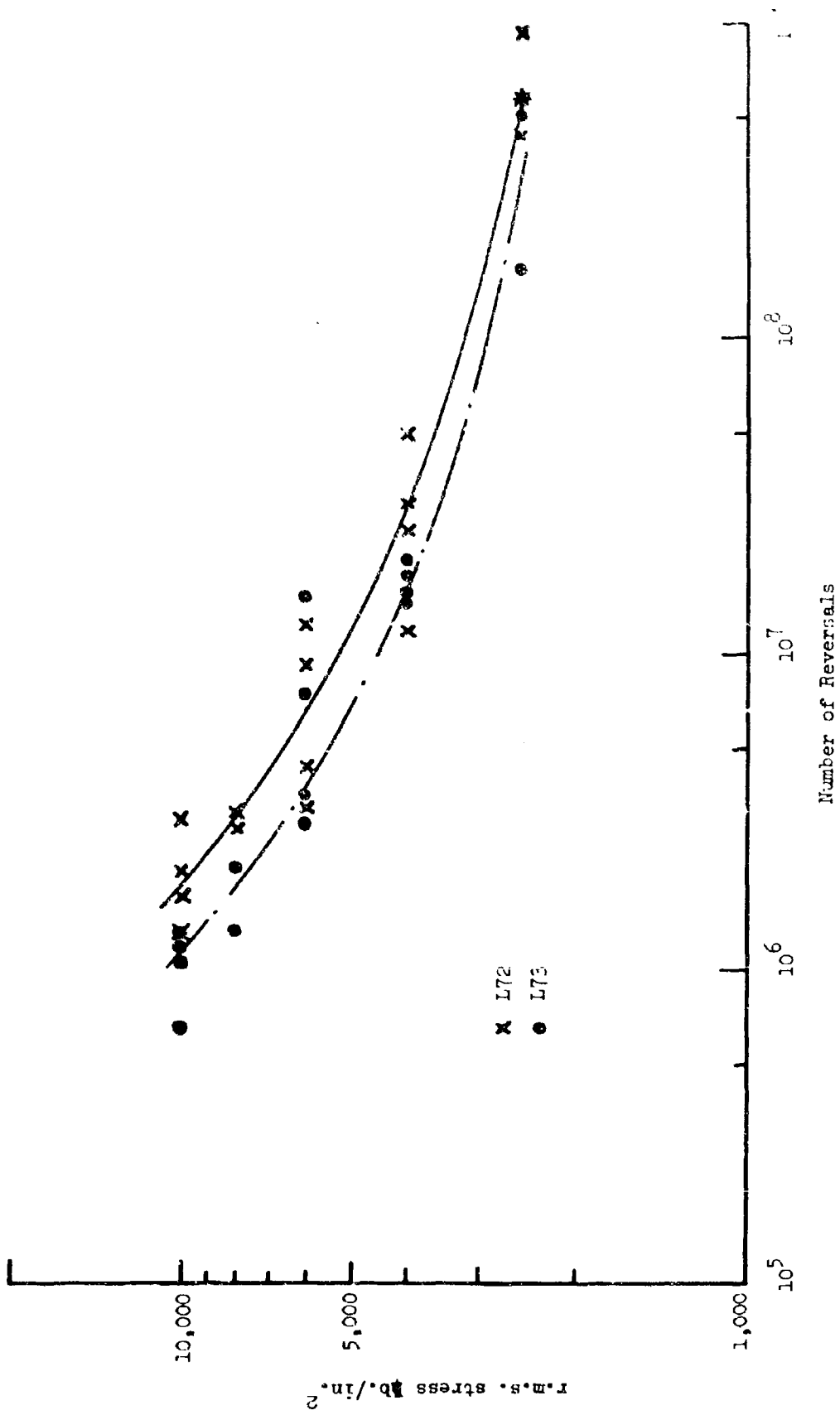FIG. 11   COMPARISON OF STRESS SPECTRA FOR RUDDER SKIN

FIG. 12 RANDOM FATIGUE DATA

DOCUMENT CONTROL DATA - R&D

(Security classification of title, body of abstract and indexing annotation must be entered when the overall report is classified)

1. ORIGINATING ACTIVITY *(Corporate author)*	2a. REPORT SECURITY CLASSIFICATION
Brian L. Clarkson Institute of Sound and Vibration Research University of Southampton	UNCLASSIFIED 2b. GROUP

3. REPORT TITLE

Stresses in Skin Panels Subjected To Random Acoustic Loading

4. DESCRIPTIVE NOTES *(Type of report and inclusive dates)*

Final Report

5. AUTHOR(S) *(Last name, first name, initial)*

Clarkson, Brian L.

6. REPORT DATE	7a. TOTAL NO. OF PAGES	7b. NO. OF REFS
June 1967	52	18

8a. CONTRACT OR GRANT NO.	9a. ORIGINATOR'S REPORT NUMBER(S)
AF61(052)-627	
b. PROJECT NO. 7351	
c.	9b. OTHER REPORT NO(S) *(Any other numbers that may be assigned this report)* AFML-TR-67-199
d.	

10. AVAILABILITY/LIMITATION NOTICES

Distribution of this document is unlimited. It may be released to the Clearinghouse, Department of Commerce, for sale to the general public.

11. SUPPLEMENTARY NOTES	12. SPONSORING MILITARY ACTIVITY
	Air Force Materials Laboratory Research and Technology Division Air Force Systems Command Wright-Patterson Air Force Base, Ohio

13. ABSTRACT

This report summarises the fully documented experimental data which is available on the stresses induced in typical aircraft structure by jet noise at take off. The experimental values are compared with a design procedure based on a single degree of freedom analysis and the method is extended for application to control surfaces and to integrally stiffened skin panels. The estimates are generally within a factor of two of the measured values. The relatively new phenomenon of shock cell noise is introduced and a typical result for the variation of r.m.s. stress during take off and climb is discussed.

DD FORM 1 JAN 64 **1473**